NASA Contractor Report 4369

A Review of Near-Wall Reynolds-Stress Closures

R. M. C. So, Y. G. Lai, H. S. Zhang,
and B. C. Hwang

GRANT NAG1-1080
MAY 1991

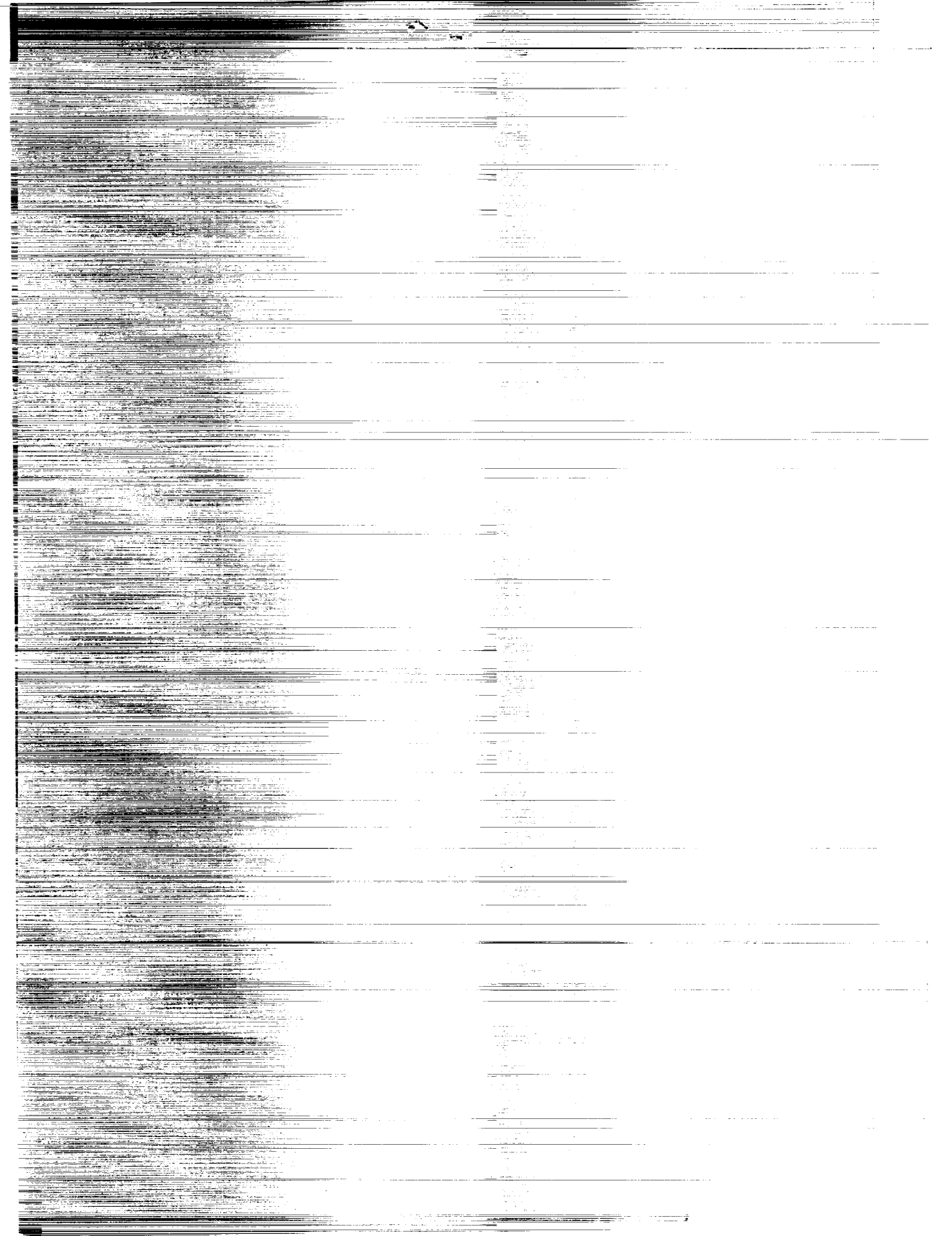

NASA Contractor Report 4369

A Review of Near-Wall Reynolds-Stress Closures

R. M. C. So, Y. G. Lai,
and H. S. Zhang
Arizona State University
College of Engineering & Applied Sciences
Tempe, Arizona

B. C. Hwang
David Taylor Research Center
Annapolis, Maryland

Prepared for
Langley Research Center
under Grant NAG1-1080

National Aeronautics and
Space Administration
Office of Management
Scientific and Technical
Information Division

1991

Abstract

This report summarizes the advances made to date in near-wall Reynolds-stress closures. All closures examined are based on some form of high-Reynolds-number models. Researchers argue that because turbulent diffusion is small near the wall, its modeling is relatively insignificant compared to viscous dissipation and velocity-pressure-gradient correlation in the near-wall region. Consequently, most near-wall closures proposed to date attempt to modify the high-Reynolds-number models for the dissipation function and the pressure redistribution term so that the resultant models are applicable all the way to the wall. Furthermore, the near-wall closures examined solve a turbulent kinetic energy dissipation-rate equation to complete the closure. Some solve the equation that governs the transport of the dissipation rate, while others solve an equation that governs the transport of the actual dissipation rate minus its wall value. Again, the high-Reynolds-number form of the equation is modified to predict the near-wall flow. The near-wall closures are examined for their asymptotic behavior so that they can be compared with the proper near-wall behavior of the exact Reynolds-stress equations. A comparison of the closures' performance in the calculation of a low-Reynolds-number plane channel flow is carried out. In addition, the closures are evaluated for their ability to predict the turbulence statistics and the limiting behavior of the structure parameters compared to direct simulation data. It is found that three near-wall Reynolds-stress closures give the best correlations with simulated turbulence statistics; however, their predictions of the near-wall Reynolds-stress budgets are incorrect. A proposed modification to the dissipation-rate equation remedies part of those predictions. Therefore, further improvements are required if a complete replication of all the turbulent properties and Reynolds-stress budgets by a statistical model of turbulence is desirable.

Contents

1. Introduction

Statistical models of turbulence have made significant advances since the mixing-length model of Prandtl[1]. This early model assumes gradient transport and prescribes, on the basis of empirical data, an algebraic behavior for the mixing length. The corresponding velocity scale is given by the product of the mixing length and the mean shear rate. Subsequent models improve on the empirical input and propose to solve either a turbulent length scale or a turbulent velocity scale equation instead of relying on a prescribed mixing length. Further improvements can be achieved by solving the length and velocity scale equations simultaneously with the mean flow equations. Consequently, the length or the velocity scale does not have to be tied to the mean shear rate. In other words, small scale turbulence is not required to have a direct link to the large scale motion. The length and velocity scale equations can be derived rigorously from the one-point statistical equations. However, in order to close these equations, the flow Reynolds number is assumed large. This assumption renders the models invalid for near-wall flows and, therefore, limits the range of applicability of the models. As a result, these so called two-equation closures are not very suitable for turbulent flows with such complexities as adverse pressure gradient, streamline curvature, fluid rotation, recirculating and reattachment behavior, etc[2].

Efforts to improve these closures have been carried out in two directions. One is to extend the two-equation closures to low-Reynolds-number flows[3]. Another is to relax the gradient transport assumption and to solve the one-point Reynolds-stress equations directly[4]. This latter approach gives rise to the commonly known Reynolds-stress or second-order closures. Again, the Reynolds-stress equations are closed by invoking the high-Reynolds-number assumption. As such, they are not valid for near-wall flows. These two improvements give mixed results[2]. However, they still fail to capture the important characteristics of near-wall turbulence[4] and the closures are performing poorly for such complex flows as turbulent curved-pipe flows[5,6]. In order to further improve the performance of second-order closures, a number of researchers have

proposed to extend the second-order closures to near-wall flows[7-15]. In general, the extension is based on well established high-Reynolds-number models for the various terms in the Reynolds-stress equations. A common approach is to modify the pressure redistribution model in order to account for the "echo" effect in the proximity of a wall[7,9,10,12]. Some of these second-order near-wall closures have been tested for a variety of simple and complex turbulent flows, and they show improvements for the flow cases that have been calculated[4,7-23]. However, the asymptotic near-wall behavior and budgets of the modelled Reynolds-stress equations have not been properly analyzed. As a result, the internal consistency of the modelled equations in the near-wall region is in doubt and needs to be analyzed and compared with the behavior and budgets of the exact Reynolds-stress equations.

With the advent of supercomputers, it is now possible to solve the Navier-Stokes equations directly to simulate turbulent flows[24-27]. As such, the statistical approach together with its inherently empirical closure assumptions becomes less attractive for turbulent flow calculations. The direct simulation approach yields turbulence results near a wall that are in excellent agreement with measurements and, for the first time, offers fluctuating pressure information that is otherwise not available from experiments[28,29]. This approach provides a powerful tool for the study of turbulent flows. At present, it is limited by flow geometries, flow Reynolds number and the speed and capacity of supercomputers. Therefore, it cannot be used to tackle such practical problems as internal flows through turbomachines. On the other hand, the turbulence information created by direct simulation of simple turbulent flows would be invaluable to turbulence modellers whose closures could be improved by incorporating this new knowledge, in particular, the pressure information, into their closure assumptions. In view of the fact that direct simulation of turbulent flows is far from being able to compete on an equal footing with turbulence modeling in terms of practical applications, it would seem prudent, at least for the near term, to make use of the simulation data to evaluate the internal consistency of second-order near-wall closures. There are nine such closures[7-15] at present. Most of these closures have not been properly analyzed for their

near-wall asymptotic behavior and their consistency with simulation results. This suggest that, before further validations and improvements of these closures are carried out, a thorough review of their ability to predict near-wall flows is beneficial.

The present objective is to review the second-order near-wall turbulence closures proposed to date. A detailed analysis of the asymptotic near-wall behavior of these closures and their comparison to simulated and measured behavior is carried out. Therefore, the relative strengths and weaknesses of the closures could be investigated and modifications proposed. It is hoped that, through this review, a physically and mathematically more consistent closure could be identified and possible improvements suggested.

2. Basic High-Reynolds-Number Models

This paper proposes to review the advances made in second-order near-wall closures. An examination of the near-wall closures[7-15] put forward to date reveal that, in one way or another, they represent extension of high-Reynolds-number closures to near-wall flows. The extensions come in different forms. However, they all involve modifying the transport equation for the dissipation rate of the turbulent kinetic energy, ε, and the models for viscous dissipation and pressure redistribution. In view of this, it would facilitate discussion of near-wall closures by first summarizing the high-Reynolds-number models used in these closures. The closure by Shih and Lumley[7] is not reviewed here, because the inner boundary conditions of their closure have to be applied at a streamline in the inertial sublayer and not at the wall. Therefore, it is different from other near-wall closures. In these other closures[8-15], the integration of the governing equations can start right from the wall and, hence, the wall boundary conditions for all turbulence quantities could be satisfied exactly. The eight near-wall closures reviewed are those proposed by Hanjalic and Launder[8], Prud'homme and Elghobashi[9], Kebede, Launder and Younis[10], So and Yoo[11], Shima[12], Launder and Tselepidakis[13], Launder and Shima[14], and Lai and So[15]. For ease of reference later, these closures are denoted by the following abbreviations; namely, HL, PE, KLY, SY, SH, LT, LSH, and LS, respectively.

The governing equations for an incompressible, stationary turbulent flow can be concisely written in Cartesian tensor as

$$\frac{\partial U_i}{\partial x_i} = 0 \quad , \tag{1}$$

$$U_k \frac{\partial U_i}{\partial x_k} = -\frac{1}{\rho}\frac{\partial P}{\partial x_i} + \frac{\partial}{\partial x_k}\left(\nu\frac{\partial U_i}{\partial x_k} - \overline{u_i u_k}\right) \quad , \tag{2}$$

where u_i and U_i are the i^{th} components of the fluctuating and mean velocity, P is mean static pressure, x_k is the k^{th} component of the Cartesian coordinates, ρ is fluid density and ν is fluid

kinematic viscosity. These equations are not closed because of the presence of the Reynolds-stress term, $-\overline{u_i u_k}$. A second-order closure of Eqs. (1) and (2) involves solving additional transport equations for the Reynolds stresses and ε. These equations can be symbolically written as:

$$C_{ij} = D_{ij}^{\nu} + D_{ij}^{T} + P_{ij} + \Phi_{ij}^{p} + \Phi_{ij} - \varepsilon_{ij} \quad , \tag{3}$$

$$C_{\varepsilon} = D_{\varepsilon}^{\nu} + D_{\varepsilon}^{T} + P_{\varepsilon} + \psi - \mathcal{D}_{\varepsilon} + \xi \quad . \tag{4}$$

The terms from left to right in (3) represent the convection, molecular diffusion, turbulent diffusion, production by mean shear, pressure diffusion, pressure redistribution, and viscous dissipation of $\overline{u_i u_j}$. Similarly, the terms in (4) represent convection, molecular diffusion, turbulent diffusion, production, extra production by mean shear, and viscous dissipation of ε. The last term ξ is usually neglected while the terms D_{ij}^{T}, Φ_{ij}, ε_{ij}, D_{ε}^{T}, P_{ε} and $\mathcal{D}_{\varepsilon}$ are modelled so that Eqs. (1) - (4) are closed. The linkage to the wall is then provided by wall function approximations, such as those proposed by Hanjalic and Launder[30] and Launder et al.[31]

All near-wall closures put forward to date except SY use a common high-Reynolds-number ε-equation. The models proposed for D_{ε}^{T}, P_{ε} and $\mathcal{D}_{\varepsilon}$ are given by $\partial[C_{\varepsilon d}(k/\varepsilon)\overline{u_k u_i}\ \partial\varepsilon/\partial x_i]/\partial x_k$, $C_{\varepsilon 1}(\varepsilon/k)\tilde{P}$ and $C_{\varepsilon 2}\varepsilon^2/k$, respectively, where $C_{\varepsilon d}$, $C_{\varepsilon 1}$ and $C_{\varepsilon 2}$ are model constants, $\tilde{P} = P_{ii}/2$ and $k = \overline{u_i u_j}/2$ is the turbulent kinetic energy. On the other hand, SY solve the transport of $\tilde{\varepsilon} = \varepsilon - 2\nu(\partial k^{1/2}/\partial x_2)^2$ rather than ε, where x_2 is normal to the wall. Thus defined, $\tilde{\varepsilon}$ goes to zero at the wall. The models they assumed for D_{ε}^{T}, P_{ε} and $\mathcal{D}_{\varepsilon}$ are $\partial[(\nu_t/\sigma_{\varepsilon})\ \partial\tilde{\varepsilon}/\partial x_k]/\partial x_k$, $C_{\varepsilon 1}(\tilde{\varepsilon}/k)\tilde{P}$ and $C_{\varepsilon 2}\tilde{\varepsilon}^2/k$, respectively, where $\nu_t = C_{\mu}k^2/\tilde{\varepsilon}$ is the eddy viscosity and σ_{ε} and C_{μ} are model constants. In this form, the equation is identical to the high-Reynolds-number form used by Chien[32].

The model used for ε_{ij} is the isotropic model of Kolmogorov[33] (hereafter denoted by KV) while the models adopted for Φ_{ij} vary from the return-to-isotropy model of Rotta[34] (hereafter denoted by RA) to the mean-strain model of Launder et al.[31] (hereafter denoted by LRR). As for

D_{ij}^T, the models proposed range from the isotropic model of Shir[35] (hereafter denoted by SR) to Daly and Harlow's model[36] (hereafter denoted by DH) to Hanjatic and Launder's model[30] (hereafter denoted by HL72). A more complicated model for D_{ij}^T has also been proposed by Cormack et al.[37] However, a later comparison of these four D_{ij}^T models by Amano and Goel[38] has shown that HL72 gives the most reasonable results among the four, even though the best result is given by solving a transport equation for the triple velocity correlation.

The different proposals adopted for D_{ij}^T, Φ_{ij} and ε_{ij} are listed in Table 1. In this tabulation, LRR1 is used to denote the LRR model without the wall pressure "echo" term while LRR2 denotes the LRR model with the "echo" term included. The modified LRR model is a different version of LRR1 with modifications made in both the turbulent and the mean-strain part. Lumley's proposal[39] to modify the turbulent part so that it goes to zero at the wall is adopted. This is accomplished by introducing a "flatness" parameter that varies from zero at a wall or an interface to one for isotropic turbulence. For completness sake, the various high-Reynolds-number models are summarized below. The turbulent diffusion models are given by:

$$SR = \frac{\partial}{\partial x_k}\left[C_\mu f_2 \frac{k^2}{\varepsilon} \frac{\partial \overline{u_i u_j}}{\partial x_k} \right] , \tag{5a}$$

$$DH = \frac{\partial}{\partial x_k}\left[C_s \frac{k}{\varepsilon} \frac{\overline{\qquad}}{u_k u_\ell} \frac{\partial \overline{u_i u_j}}{\partial x_\ell} \right] , \tag{5b}$$

$$HL72 = \frac{\partial}{\partial x_k}\left[C_s \frac{k}{\varepsilon} \left(\overline{u_k u_\ell} \frac{\partial \overline{u_i u_j}}{\partial x_\ell} + \overline{u_j u_\ell} \frac{\partial \overline{u_k u_i}}{\partial x_\ell} + \overline{u_i u_\ell} \frac{\partial \overline{u_j u_k}}{\partial x_\ell} \right) \right] . \tag{5c}$$

The dissipation model is adopted from Kolmogorov[33], or

$$KV = \frac{2}{3}\delta_{ij}\,\varepsilon . \tag{6}$$

Finally, the different models proposed for Φ_{ij} are:

$$RA = - C_1 \frac{\varepsilon}{k}\left(\overline{u_i u_j} \quad - \quad \frac{2}{3}\delta_{ij}k\right) \quad , \tag{7a}$$

$$LRR1 = RA + \Phi_{ij,2} = RA - \alpha_1\left(P_{ij} - \frac{2}{3}\delta_{ij}\,\tilde{P}\right) - \beta_1\left(D_{ij} - \frac{2}{3}\,\delta_{ij}\,\tilde{P}\right) - \gamma_1\, k\, S_{ij} \quad , \tag{7b}$$

$$LRR2 = LRR1 + C_1^{'}\frac{\varepsilon}{k}\left[\overline{u_k u_m} n_k n_m \delta_{ij} - \frac{3}{2}\overline{u_k u_i}\, n_k n_j - \frac{3}{2}\overline{u_k u_j}\, n_k n_i\right]\left(\frac{C_3^{'} k^{3/2}}{\varepsilon y}\right)$$

$$+ C_2^{'}\left[\Phi_{km,2} n_k n_m \delta_{ij} - \frac{3}{2}\Phi_{ik,2} n_k n_j - \frac{3}{2}\Phi_{jk,2} n_k n_i\right]\left(\frac{C_3^{'} k^{3/2}}{\varepsilon y}\right) \quad , \tag{7c}$$

$$\text{modified LRR} = C_1 (AA_2)^{1/2}\varepsilon\left|a_{ij} + 1.1\left[a_{ik}a_{kj} - \frac{1}{3}\delta_{ij}A_2\right]\right| - a_{ij}\varepsilon - 0.6\left(P_{ij} - \frac{2}{3}\delta_{ij}\tilde{P}\right)$$

$$+ 0.6\varepsilon\, a_{ij}\left(\frac{\tilde{P}}{\varepsilon}\right) - 0.2\left[\frac{\overline{u_k u_j}\,\overline{u_\ell u_i}}{k} S_{k\ell} - \frac{\overline{u_\ell u_k}}{k}\left\{\overline{u_i u_k}\frac{\partial U_j}{\partial x_\ell} + \overline{u_j u_k}\frac{\partial U_i}{\partial x_\ell}\right\}\right]$$

$$-0.6\left[(A_2 (P_{ij} - D_{ij}) + 3\, a_{mi}a_{nj}\,(P_{mn} - D_{mn})\right] \quad . \tag{7d}$$

In these equations

$$P_{ij} = -\left[\overline{u_i u_k}\frac{\partial U_j}{\partial x_k} + \overline{u_j u_k}\frac{\partial U_i}{\partial x_k}\right] \quad ,$$

$$D_{ij} = -\left[\overline{u_i u_k}\frac{\partial U_k}{\partial x_j} + \overline{u_j u_k}\frac{\partial U_k}{\partial x_i}\right] \quad ,$$

$$S_{ij} = \left[\frac{\partial U_i}{\partial x_j} + \frac{\partial U_j}{\partial x_i}\right] \quad ,$$

$$a_{ij} = \left[\frac{\overline{u_i u_j}}{k} - \frac{2}{3}\,\delta_{ij}\right] \quad ,$$

$$f_2 = 1 - \exp\left[-C_3\, u_\tau\, y/\nu\right] \quad ,$$

$$A_2 = a_{ij}\, a_{ij} \quad ,$$

$$A_3 = a_{ij}\, a_{jk}\, a_{ki} \quad ,$$

$$A = 1 - 9\,(A_2 - A_3)/8 \quad ,$$

$n_i = (0, 1, 0)$ is a unit normal vector and C_1, $C_1^{'}$, $C_2^{'}$, C_3, $C_3^{'}$, C_s, α_1, β_1 and γ_1 are model constants. The three constants α_1, β_1 and γ_1 are not independent, rather they are related to a constant C_2. The exact relations are given in Ref. 31. Different researchers adopt different values for the model constants. Therefore, the readers are advised to refer to the original papers for their chosen values. It should be pointed out that ε should be replaced by $\tilde{\varepsilon}$ in all the above models when they are used in SY.

It is obvious from this compilation that the high-Reynolds-number versions of these near-wall closures are very similar. They all used KV to model ε_{ij} and essentially different versions of LRR to model Φ_{ij}. The difference in the modeling of D_{ij}^{T} is slight and, as pointed out by Launder et al.[31], is insignificant. As a result, all these closures can be expected to perform well far away from a wall for a wide variety of turbulent flows because they are basically similar to the second-order high-Reynolds-number closure put forward by Launder et al.[31]

3. Near-Wall Behavior of the Reynolds Stresses

Sufficient data are now available to establish the following relations for the Reynolds stresses in the near-wall region. These data are obtained from direct simulation of a plane channel flow[25] and from two-dimensional channel[40-45], pipe[46,47] and flat plate boundary layer experiments[48]. If u^+_{rms}, v^+_{rms}, w^+_{rms}, k^+ and $-\overline{uv}^+$ are used to denote $(\overline{u^2}/u_\tau^2)^{1/2}$, $(\overline{v^2}/u_\tau^2)^{1/2}$, $(\overline{w^2})/u_\tau^2)^{1/2}$, k/u_τ^2 and $-\overline{uv}/u_\tau^2$, then the Reynolds stresses, assuming incompressible flow, in the near-wall region can be expressed in terms of y^+ as:

$$u^+_{rms} = a_u y^+ + b_u y^{+2} + \dots \ , \tag{8a}$$

$$v^+_{rms} = a_v y^{+2} + b_v y^{+3} + \dots \ , \tag{8b}$$

$$w^+_{rms} = a_w y^+ + b_w y^{+2} + \dots \ , \tag{8c}$$

$$k^+ = a_k y^{+2} + b_k y^{+3} + \dots \ , \tag{8d}$$

$$-\overline{uv}^+ = a_{uv} y^{+3} + b_{uv} y^{+4} + \dots \ , \tag{8e}$$

where u_τ is the wall friction velocity, u, v and w are the fluctuating velocity components along the stream (x), the normal (y) and the transverse (z) direction, the a's and b's are constants for fully-developed turbulent flows, and $y^+ = yu_\tau/\nu$. The leading coefficients of (8) can be determined from existing data[25,40-45] by examining the behavior of the Reynolds stresses in the region, $0 \le y^+ < 10$. Whenever possible, mean lines through the data are used to approximate the behavior near the wall. The results thus obtained are tabulated in Table 2 together with the maximum values of u^+_{rms}, v^+_{rms}, w^+_{rms}, k^+ and $-\overline{uv}^+$ (denoted by a subscript m) and their respective locations (denoted by $(y^+)_m$). The Reynolds number Re is based on centerline velocity and channel width (or pipe diameter).

From this tabulation, it can be seen that there is a lot of scatter between the various measurements. For example, a_u varies from a low of 0.24 to a high of 0.45 with an average value of ~ 0.35. It is now known that the measurements of Eckelmann[40] and Kreplin and Eckelmann[42] are not accurate in the near-wall region because they have not corrected their hot-wire outputs for wall proximity effects. The measurements of Kasagi et al.[49] are similar to those of Ref. 29 because their hot-film outputs are also not corrected for wall influences. Furthermore, the measurements of Sirkar and Hanratty[50] give an $a_k = 0.05$, while the data collected by Derksen and Azad[51] give a range of 0.025 to 0.05 for a_k. These values are substantially lowered than those reported by Kim et al.[25] and Nishino and Kasagi[45]. Some of the discrepancies are due to difference in Re. However, according to the analysis of Nishino and Kasagi[45], it seems that most hot-wire or hot-film measurements are affected by various error sources in the near-wall region. Some errors, like heat conduction and natural convection effects, could be corrected but others are unaccountable. As a result, the hot-wire or hot-film data are not as accurate as the particle tracking measurements of Ref. 45. Since the data of Ref. 45 are in close agreement with the simulation result[25], it would seem that these two sets of data are most suitable for validating second-order near-wall closures.

The dissipation rate of k is defined as

$$\varepsilon = \nu \overline{\left(\frac{\partial u_i}{\partial x_k}\right)\left(\frac{\partial u_i}{\partial x_k}\right)} \quad . \tag{9}$$

If the expansions

$$u = a_1 y + a_2 y^2 + \dots \ , \tag{10a}$$

$$v = b_1 y + b_2 y^2 + \dots \ , \tag{10b}$$

$$w = c_1 y + c_2 y^2 + \dots \ , \tag{10c}$$

where $a_i(x,z,t)$, $b_i(x, z, t)$ and $c_i(x, z, t)$ are random functions, are assumed in the near-wall region, then continuity requires $b_1 \equiv 0$. A simple manipulation of (10) then gives $a_k = \nu^2(\overline{a_1^2} + \overline{c_1^2})/2u_\tau^4$ and $b_k = \nu^3\left(\overline{a_1 a_2} + \overline{c_1 c_2}\right)/u_\tau^5$, where the overbar is used to denote time average. Substituting (10) into (9) gives the near-wall behavior of ε and the result is

$$\varepsilon^+ = 2a_k + 4b_k\, y^+ + \ldots \quad , \tag{11}$$

where $\varepsilon^+ = \varepsilon\nu/u_\tau^4$. Therefore, the limiting wall value of ε is $\varepsilon^+ = 2a_k$ and its slope at the wall is given by $4b_k$. In view of this, it is important to determine the coefficients a_k and b_k correctly. Nishino and Kasagi[45] give a $b_k = -\,8.4 \times 10^{-3}$. They have also determined the b coefficients for the other Reynolds stresses. For completness sake, these values are quoted here as $b_u = -\,0.21$, $b_v = -5.03 \times 10^{-4}$, $b_w = -0.010$ and $b_{uv} = -\,4.9 \times 10^{-5}$. The negative b_k value indicates that $-\varepsilon$ decreases away from the wall. In other words, $-\varepsilon$ reaches a maximum at the wall. This trend is consistent with direct simulation results[26]. In view of the small value of b_k, it is rather inaccurate to try to determine b_k from the simulation data[25]. Nevertheless, an attempt has been made and the value so determined is $b_k = -6.6 \times 10^{-3}$, which is in fair agreement with that reported in Ref. 45. Therefore, the slope of ε^+ at the wall is $4b_k = -0.0264$ and is not so small as to be negligible. Consequently, the assumption that $\partial\varepsilon^+/\partial y^+ = 0$ at the wall is incorrect and cannot be used as a boundary condition for ε as suggested in Ref. 3. The correct boundary condition should be $\varepsilon^+ = 2a_k$. In general, a_k is not known a prior. However, since $\partial\sqrt{k^+}/\partial y^+ = \sqrt{a_k}$, this suggests that an alternative boundary condition could be $\varepsilon^+ = 2(\partial\sqrt{k^+}/\partial y^+)^2$, a condition first derived by Jones and Launder[52]. Similarly, $k^+/y^{+2} = a_k$, therefore, $\varepsilon^+ = 2k^+/y^{+2}$ could also be used as a boundary condition. This means that $k^+/y^{+2}\varepsilon^+$ is exactly 0.5 and could be used to assess the closures' ability to replicate near-wall flows. The b_k value thus determined plus the values for the coefficient "a" listed in Table 2 and the $k^+/y^{+2}\varepsilon^+$ value are used to assess the internal consistency of the eight second-order near-wall closures.

Finally, in the near-wall region, the dissipation function ε_{ij} and the Reynolds stresses $\overline{u_i u_j}$ have to asymptote correctly to the following ratios[53]; namely,

$$\frac{\varepsilon_{11}}{\overline{u^2}} = \frac{\varepsilon_{33}}{\overline{w^2}} = \frac{\varepsilon_{13}}{\overline{uw}} = \frac{\varepsilon}{k} \ , \tag{12a}$$

$$\frac{\varepsilon_{23}}{\overline{vw}} = \frac{\varepsilon_{12}}{\overline{uv}} = \frac{2\varepsilon}{k} \ , \tag{12b}$$

$$\frac{\varepsilon_{22}}{\overline{v^2}} = \frac{4\varepsilon}{k} \ . \tag{12c}$$

Furthermore, ε_{ij} has to contract to 2ε, otherwise (9) will not be satisfied. Here, 1 denotes the stream or x-direction, 2 and 3, the normal and transverse directions, respectively. Together, (8), (11) and (12) define the correct asymptotic behavior for $\overline{u_i u_j}$, k, ε and ε_{ij} in the near-wall region. The validity of any second-order near-wall closure should be judged by its ability to mimic these characteristics, especially when its basic high-Reynolds-number model has been extensively verified as in the eight cases listed in Table 1.

4. Near-Wall Reynolds-Stress Closures

With this understanding of the near-wall behavior of the Reynolds stresses, the improvements made by various researchers to model near-wall turbulence can now be discussed. It should be pointed out that since the terms D^{ν}_{ij} and D^{ν}_{ε} do not need modeling they are included in all near-wall modelled equations. In other words, (3) and (4) are solved without neglecting D^{ν}_{ij} and D^{ν}_{ε} in these equations. With the exception of LSH and LS, all near-wall closures examined neglect Φ^{p}_{ij}, or, it can be said that pressure diffusion effects are being modelled together with D^{T}_{ij} by such models as SR, DH and HL72. Recognizing the importance of pressure diffusion in the near-wall region[28,29], LSH and LS attempt to incorporate this effect into the closure by considering the modeling of the velocity-pressure-gradient correlation rather than pressure redistribution alone in the near-wall region. Consequently, the models that need modifications are those associated with D^{T}_{ij}, Φ^{p}_{ij}, Φ_{ij}, and ε_{ij}.

HL Closure[8]

HL argue that, at least to the lowest order, ν does not appear in Φ_{ij}. Therefore, the model for Φ_{ij} need not be modified for near-wall viscous effects. They also argue that, for $y^+ < 15$, the effects of diffusive transport on the stress budgets are insignificant. In other words, HL72 can be used without modification. This only leaves ε_{ij} for modification. They argue that as the Reynolds number approaches zero, the energy-containing and dissipation range of motions overlap and ε_{ij} could be approximated by $\varepsilon_{ij} = \overline{u_i u_j}\,(\varepsilon/k)$[34]. Consequently, they propose to modify ε_{ij} by

$$\varepsilon_{ij} = \frac{2}{3}\varepsilon\left[(1 - f_s)\delta_{ij} + \frac{\overline{u_i u_j}}{(2k/3)} f_s\right] , \tag{13}$$

where $f_s = (1 + R_T/10)^{-1}$ and $R_T = k^2/\nu\varepsilon$. This ε_{ij} model contracts to 2ε everywhere in the flow. They further modify their ε-equation by defining the term $\mathcal{D}_{\varepsilon}$ as $C_{\varepsilon 2} f_{\varepsilon}\, \varepsilon\tilde{\varepsilon}/k$, where $f_{\varepsilon} = 1 - (2/9)\exp[-(R_T/6)^2]$. By introducing $\tilde{\varepsilon}$ to replace one of the ε in $\mathcal{D}_{\varepsilon}$, the term approaches zero at the wall

by virtue of (8) and (11). In addition, they neglect the effect of ξ and model the extra production term in the ε-equation to account for mean-strain generation of ε, or

$$\psi = C_{\varepsilon 3}\, \nu \frac{k}{\varepsilon} \overline{u_j u_k} \left(\frac{\partial^2 U_i}{\partial x_j \partial x_\ell}\right)\left(\frac{\partial^2 U_i}{\partial x_k \partial x_\ell}\right) \quad . \tag{14}$$

PE Closure[9]

PE propose to modify the high-Reynolds-number model for D_{ij}^T by multiplying it by $f_\mu = \exp\,[-3.4\,(1 + R_T/50)^{-2}]$. They adopt a form for ε_{ij} very similar to (13), but with minor changes. The rationale is to provide better representation of the anisotropy of the normal stresses. Their model is given by

$$\varepsilon_{ij} = \frac{2}{3}\delta_{ij}\,\varepsilon + \frac{\varepsilon}{k}\overline{u_i u_j}\;(1 - \delta_{ij})\, f_s \tag{15}$$

where the summation convention does not apply. This modification does not allow ε_{ij} to contract to 2ε near a wall. To further account for normal stress anisotropy near a wall, they propose to add a term,

$$\Phi_{ij,w} = C_3\,(P_{ij} - D_{ij})\,\exp\,\{-C_4\, k^{1/2} y/\nu], \tag{16}$$

to Φ_{ij}. Consequently, their near-wall model for Φ_{ij} is given by (LRR1 + $\Phi_{ij,w}$). The models they used to modify the ε-equation are similar to those of HL with two exceptions. In their case, the extra term ψ is given by

$$\psi = 2\nu(k/\nu) f_\mu\, \overline{u_j u_k} \left(\frac{\partial^2 Ui}{\partial x_j \partial x_\ell}\right)\left(\frac{\partial^2 Ui}{\partial x_k \partial x_\ell}\right) \quad , \tag{17}$$

and the high-Reynolds-number model for $\mathcal{D}_\varepsilon$ is modified by f_μ.

KLY Closure[10]

This closure is similar to that of HL, with two exceptions. One is the high-Reynolds-number model adopted for Φ_{ij}. They use LRR2 which include the wall pressure "echo" term.

Another is the model proposed for ε_{ij}. They point out that (13) does not satisfy the kinematic conditions (12) and proceed to propose

$$\varepsilon_{ij} = \frac{2}{3}\delta_{ij}\varepsilon(1 - f_s) + \frac{\varepsilon}{k} f_s F\left[\overline{u_i u_j} + \overline{u_i u_k}\, n_k n_j + \overline{u_j u_k}\, n_k n_i + \delta_{ij}\,\overline{u_k u_\ell} n_k n_\ell\right] , \qquad (18)$$

to replace (13). This modification satisfies (12), but it does not contract properly to 2ε if F is taken to be unity. However, its proper contraction is assured if $F = (1 + 2.5\,\overline{v^2}/k)^{-1}$ is assumed. Here, f_s is defined differently and is given by $f_s = \exp[-R_T/40]$. The ε-equation used is identical to that of HL.

SY Closure[11]

SY essentially follow the arguements of HL and suggest the modification of ε_{ij} only. Their concern is to make the governing equations balance, at least to the lowest order of y, near a wall. As a result, they adopt Chien's low-Reynolds-number ε-equation[32] which neglects ψ and proposes to model ξ by

$$\xi = -\frac{2\nu\tilde{\varepsilon}}{y^2}\exp[-C_4 y u_\tau/\nu] \qquad (19)$$

to account for near-wall viscous effects. Chien also defines $D_\varepsilon^T = \partial[(\nu_t/\sigma_\varepsilon)\,(\partial\tilde{\varepsilon}/\partial x_k)]/\partial x_k$, where $\nu_t = C_\mu(k^2/\tilde{\varepsilon})f_2$. With this definition for ν_t, the model requires $\tilde{\varepsilon}$ to behave like y^2 near a wall, instead of y as suggested by (11). Nevertheless, this behavior renders the models for Φ_{ij} to vanish at the wall and allows SY to modify ε_{ij} only. Their proposal is

$$\varepsilon_{ij} = \frac{2}{3}\delta_{ij}\tilde{\varepsilon} + \frac{2\nu\,\delta_{i\ell}\,\delta_{jm}\,\overline{u_\ell u_m}}{y^2} . \qquad (20)$$

One drawback of this model is that it does not contract properly to 2ε. However, the closure equations do have the advantage of remaining in balance as a wall is approached.

SH Closure[12]

SH follows the arguements of Lumley[54] to rearrange Φ_{ij} and ε_{ij}. Instead of modeling these two terms separately, the treatment re-writes them into

$$-\varepsilon_{ij} + \Phi_{ij} = -\frac{2}{3}\delta_{ij}\varepsilon + \left[\Phi_{ij,1} - \varepsilon_{ij} + \frac{2}{3}\delta_{ij}\varepsilon\right] + \Phi_{ij,2}, \tag{21}$$

where $\Phi_{ij} = \Phi_{ij,1} + \Phi_{ij,2}$ and $\Phi_{ij,1}$ represents the turbulent part and $\Phi_{ij,2}$ the mean-strain part of Φ_{ij}. This way, SH does not have to model ε_{ij}. He proposes to model the square bracketed term in (21) by the RA model except that C_1 is replaced by $C_1[1-(1-1/C_1)f_w]$, where $f_w = \exp[-(0.015k^{1/2}y/\nu)^4]$ is specified. The term $\Phi_{ij,2}$ is given by (7b). In addition, SH proposes a near-wall correction to (21) given by

$$\Phi_{ij,w} = f_w\left[0.45\left(P_{ij} - \frac{2}{3}\delta_{ij}\tilde{P}\right) - 0.03\left(D_{ij} - \frac{2}{3}\delta_{ij}\tilde{P}\right) + 0.08kS_{ij}\right] \quad . \tag{22}$$

The ε-equation is modelled by first analysing its near-wall behavior using (8d) and (11). This results in a term of

$$\xi = \left[\left(-2 + \frac{7}{9}C_{\varepsilon 2}\right)\frac{\varepsilon\tilde{\varepsilon}}{k} - \frac{\overline{\varepsilon}^2}{2k}\right]f_w \tag{23}$$

to effect balance of the ε-equation in the near-wall region, after replacing $C_{\varepsilon 2}\varepsilon^2/k$ by $C_{\varepsilon 2}\,\varepsilon\tilde{\varepsilon}/k$. Here, $\overline{\varepsilon}$ is defined by SH to be $\overline{\varepsilon} = \varepsilon - \nu\partial^2 k/\partial x_i \partial x_i$. As for ψ, SH lumps it together with P_ε and proposes

$$P_\varepsilon + \psi = C_{\varepsilon 1}(1 + f_w)\frac{\varepsilon}{k}\tilde{P} \quad . \tag{24}$$

In view of the definition of $\overline{\varepsilon}$, the boundary condition for ε becomes $\varepsilon = \nu\partial^2 k/\partial x_i \partial x_i$ at the wall.

It should be pointed out that even though Shima[12] proposed to model $\Phi_{ij,w}$ with three terms on the right hand side of (22), he actually neglected the second term within the square

bracket in his closure calculations. His justification was that it is relatively small compared to the first term. In view of this, the SH model used in the present calculations is the final model adopted by Shima; that is, (22) is implemented without the second term in the square bracket.

LT Closure[13]

This closure adopts (18) for ε_{ij} to account for near-wall viscous effects and an identical ε-equation to that proposed by KLY. Therefore, the only difference between LT and KLY is in the modeling of Φ_{ij}. KLY use (7c) for Φ_{ij} while LT use (7d).

LSH Closure[14]

This closure adopts an approach similar to that of SH and proposes only to modify Φ_{ij}. The modifications implement the suggestion of Lumley[39], so that the resultant Φ_{ij} vanishes at the wall. Instead of just varying C_1 to accomplish this objective, LSH propose to modify the constants C_1, C_2, C_1' and C_2' in LRR2 by

$$C_1 = 1 + 2.58\, AA_2^{1/4}\, [1-\exp\{-(0.0067R_T)^2\}] \quad , \tag{25a}$$

$$C_2 = 0.75\, A^{1/2} \quad , \tag{25b}$$

$$C_1' = -\frac{2}{3} C_1 + 1.67 \quad , \tag{25c}$$

$$C_2' = \max\left[\left(\frac{2}{3} C_2 - \frac{1}{6}\right)/C_2,\ 0\right] \quad . \tag{25d}$$

As for the ε-equation, ξ is assumed to be zero and ψ is taken to be given by $\Psi = (\Psi_1 + \Psi_2)\frac{\varepsilon}{k}\widetilde{P}$, where

$$\Psi_1 = 2.5A\left(\frac{\widetilde{P}}{\varepsilon} - 1\right) \quad , \tag{26a}$$

$$\Psi_2 = 0.3(1 - 0.3A_2)\exp[-(0.002R_T)^2] \quad . \tag{26b}$$

LS Closure[15]

The rationale behind the derivation of this closure is essentially similar to that used in SY, namely, the first and foremost concern is to effect a balance of the modelled equations in the near-wall region. While SY carry this out to $O(y^2)$ for the 22 component, LS carry out the balance to $O(y^3)$ because the direct simulation results[25,26] show that pressure diffusion along the 22 component is important near a wall. In (3), the term $(\Phi_{ij}^p + \Phi_{ij})$ vanishes at the wall for all components while the term Φ_{ij} does not. Consequently, LS propose to model $(\Phi_{ij}^p + \Phi_{ij})$ in such a way that the model approaches LRR1 far away from the wall. This is accomplished by adding a term $\Phi_{ij,w}$ to LRR1, where

$$\Phi_{ij,w} = \left[C_1 \left(\frac{\varepsilon}{k} \overline{u_i u_j} - \frac{2}{3} \delta_{ij} k \right) - \frac{\varepsilon}{k} \left(\overline{u_i u_k} n_k n_i + \overline{u_j u_k} n_k n_i \right) + \alpha^* \left(P_{ij} - \frac{2}{3} \delta_{ij} \tilde{P} \right) \right] f_{w,1}, \quad (27)$$

and $f_{w,1} = \exp[-(R_T/150)^2]$. Furthermore, ε_{ij} is modelled in a manner similar to KLY and the resultant model is given by

$$\varepsilon_{ij} = \frac{2}{3}\varepsilon (1 - f_{w,1}) \delta_{ij} + f_{w,1} \frac{\varepsilon}{k} \left[\overline{u_i u_j} + \overline{u_i u_k} n_k n_j + \overline{u_j u_k} n_k n_i + n_i n_j \overline{u_k u_\ell} n_k n_\ell \right] \Big/$$

$$\left[1 + \frac{3 \overline{u_k u_\ell} n_k n_\ell}{2k} \right] . \quad (28)$$

The ε-equation is modified similarly to that of SH so that $\partial\varepsilon/\partial t$ is required to have the proper behavior at the wall. LS propose to model $(\psi + C_{\varepsilon 1} \tilde{P}\varepsilon/k)$ by $C_{\varepsilon 2} (1 + \sigma f_{w,2})\varepsilon\tilde{P}/k$, where σ depends on Re as a result of the direct simulation study of Mansour et al.[55] The expression suggested by LS for σ is $\sigma = [1.0 - 0.6\exp(-Re/10^4)]$. Here, $f_{w,2}$ is given by $f_{w,2} = \exp[-(R_T/64)^2]$. Furthermore, LS propose the following expression for ξ, namely,

$$\xi = f_{w,2} \left[\left(\frac{7}{9} C_{\varepsilon 2} - 2 \right) \frac{\varepsilon\tilde{\varepsilon}}{k} - \frac{\varepsilon^{*2}}{2k} \right] , \quad (29)$$

where $\varepsilon^* = \varepsilon - 2\nu k/y^2$. This way, the wall boundary condition for ε is $2\nu(\partial\sqrt{k}/\partial y)^2$ and the ε-equation still asymptote correctly at the wall as suggested by SH.

5. Near-Wall Asymptotic Behavior of the Closures

In order to analyse the near-wall asymptotic behavior of each closure, expansions (10) are assumed for u_i. Similar expansions can also be assumed for U_i. From the definitions of k and ε, the use of (10) leads to

$$k = \frac{1}{2} A_1 y^2 + B_1 y^3 + E_1 y^4 + \ldots \quad , \tag{30a}$$

$$\varepsilon = \nu A_1 + 4\nu B_1 y + \nu F_1 y^2 + \ldots \quad , \tag{30b}$$

where $A_1 = (\overline{a_1^2} + \overline{c_1^2})$, $B_1 = (\overline{a_1 a_2} + \overline{c_1 c_2})$, $E_1 = \overline{a_2^2} + 2\overline{a_1 a_3} + \overline{b_2^2} + \overline{c_2^2} + 2\overline{c_1 c_3}$ and F_1, besides being functions of the statistics of a_1 and c_1, is also functions of the derivatives of a_1 and c_1. Furthermore, if (10) and the expansions for U_i are substituted into (3), it can be easily shown that the lowest order term among the different components of C_{ij}, D_{ij}^T and P_{ij} is $O(y^3)$. Therefore, to $O(y^2)$, they do not affect the balance of (3) in the near-wall region. The analyses of the terms D_{ij}^ν, $(\Phi_{ij}^p + \Phi_{ij})$ and ε_{ij} show that the lowest order term in $(\Phi_{22}^p + \Phi_{22})$ has to be $O(y^2)$ in order to balance the term $(D_{ij}^\nu - \varepsilon_{ij})$ to this order, and the lowest order term in the other components of $(\Phi_{ij}^p + \Phi_{ij})$ has to be $O(y)$ in order to balance the same components of $(D_{ij}^\nu + \varepsilon_{ij})$ to $O(y)$. This means that all the terms in (3) vanish at the wall. Therefore, the modelled form of (3) should also possess this basic property.

Using expansions (10) and (30), the various turbulent diffusion models (5) can be analysed for their near-wall behavior. With the exception of SY, the asymptotic behavior of k/ε is given by $(y^2/2\nu) + O(y^3)$ and $k^2/\varepsilon = A_1 y^4/4\nu + O(y^5)$. Consequently, the lowest order term among the components in DH and HL72 is $O(y^6)$ and in SR is $O(y^5)$. As for SY, $\tilde{\varepsilon}$ is solved instead of ε. Also, $\tilde{\varepsilon}$ is required to behave like y^2 near a wall[32]. This leads to a behavior of $O(y^o)$ for $k/\tilde{\varepsilon}$ and $O(y^2)$ for $k^2/\tilde{\varepsilon}$. Therefore, the lowest order term among the components of SR is $O(y^2)$. The corresponding behavior for DH and HL72 is $O(y^4)$. In other words, the asymptotic behavior of all

diffusion models is not correct compared to the original behavior of D_{ij}^T. Nevertheless, with the exception of SR used in SY, the lowest order term among the different components of the various diffusion models is $O(y^4)$, which is smaller than $O(y^3)$ for D_{ij}^T. This means that in the asymptotic analysis of the modelled form of (3), only the term D_{ij}^ν and the models for $(\Phi_{ij}^p + \Phi_{ij})$ and ε_{ij} need be considered. The result of this analysis is tabulated in Table 3 together with the behavior of the exact term given by $(D_{ij}^\nu + \Phi_{ij}^p + \Phi_{ij} - \varepsilon_{ij})$. In this tabulation, the lowest order term in each component of the modelled and exact form of $(D_{ij}^\nu + \Phi_{ij}^p + \Phi_{ij} - \varepsilon_{ij})$ is listed.

From this tabulation, it can be seen that SY, SH, LSH and LS satisfy the basic requirement that the modelled Reynolds-stress equations vanish at the wall. This is accomplished without imposing any constraints on the behavior of the random functions a_i, b_i and c_i. PE also satisfies the requirement for all components except 13 if C_1 is taken to be unity, a condition correctly pointed out by Launder and Shima[14]. However, C_1 is chosen to be 1.17 in PE. It should be pointed out that the 11, 33, 13 and 22 components of SH and LSH vanish at the wall as a result of setting $C_1 = 1$ as suggested by Launder and Shima[14]. As for HL and KLY, the 11, 33, 13 and 22 components do not vanish at the wall even when $C_1 = 1$ is assumed. This is also true of the 13 component of PE. The 11, 33, 13 and 22 components of LT are also finite at the wall irrespective of the value of C_1. However, these expressions are too cumbersome to be listed explicitly in Table 3. It should be noted that all the finite expressions listed in Table 3 involve the time-averaged correlations of the random functions a_i, b_i and c_i. Since the equations have to remain balance at the wall, certain constraints would have to be imposed by the HL, PE, KLY and LT models on the random functions a_i, b_i and c_i so that the 11, 33, 13 and 22 components would go to zero at the wall. Therefore, this means that the near-wall turbulence statistics would be required to behave in a certain manner that might or might not be correct. Furthermore, according to the asymptotic analysis of (3), the lowest order term of $(D_{ij}^\nu + \Phi_{ij}^p + \Phi_{ij} - \varepsilon_{ij})$ for the 11, 33 and 13 components is $O(y^3)$, while that for the 12 and 23 components is $O(y^4)$ and that for the 22 component is $O(y^5)$ (see Table 3). In this analysis, the $\partial/\partial t$ term in (3) is neglected because of the stationarity

assumption. The closures, SY, SH, LSH and LS, give an incorrect asymptotic behavior for all six components. However, LS tries to match the 12, 23 and 22 components to a higher order of y in the hope that the resultant closure could predict more correctly the anisotropic behavior of the normal stresses in the near-wall region.

The failure of the closures to make the 11, 33, 13 and 22 components of $(D^{\nu}_{ij} + \Phi^{p}_{ij} + \Phi_{ij} - \varepsilon_{ij})$ vanish at the wall without imposing contraints on the model constants and/or the random functions could be traced to the incorrect modeling of Φ_{ij} or ε_{ij}. Since departures from local anisotropy are indistinguishable from contributions to the process of Φ_{ij} or ε_{ij}, it follows that either or both processes could be modelled in such a way that the resultant term $(D^{\nu}_{ij} + \Phi^{p}_{ij} + \Phi_{ij} - \varepsilon_{ij})$ vanishes at the wall for all i's and j's. After all, the original term does vanish at the wall for all components. This arguement is used in SY to accomplish the desire objective, however, at the expense of solving a pseudo dissipation-rate equation. In HL, ε_{ij} is not modified to compensate for the incorrect asymptotic behavior of LRR1. Rather, it is modified to approximate the behavior of ε_{ij} as Reynolds number goes to zero. Consequently, the incorrect asymptotic behavior of LRR1 remains in the closure. The same can also be said of PE and KLY. Even though these closures add a $\Phi_{ij,w}$ term to their Φ_{ij} model, the rationale is to account for the "echo" effect of pressure fluctuations near a wall. No consideration has been given to partially compensate for the neglected pressure diffusion effect and, thus, to reproduce the correct asymptotic behavior for $(D^{\nu}_{ij} + \Phi^{p}_{ij} + \Phi_{ij} - \varepsilon_{ij})$. SH and LSH recognize this shortcoming and the suggestion of Lumley[39] is applied to remedy the incorrect asymptotic behavior of LRR1. Even then, the behavior of the 12 and 23 components is correct to O(y) only while the 22 component is correct to $O(y^2)$. This behavior is not quite consistent with the original behavior of the $\overline{u_i u_j}$ equations. In LS, a special attempt has been made to cancel out the incorrect asymptotic behavior of LRR1 near a wall. The result is a $\Phi_{ij,w}$ proposal that partially models Φ^{p}_{ij} near a wall, while at the same time compensates for the non-zero wall components of LRR1, so that the resultant modelled components of $(\Phi^{p}_{ij} + \Phi_{ij})$

vanish at the wall. This way, the behavior of the 12 and 23 components is improve to $O(y^2)$ and that of the 22 component to $O(y^3)$.

All the dissipation-rate equations used approach their respective boundary conditions correctly at the wall. However, not all equations satisfy the additional wall condition found to be important by Shima[12]. This condition is the coincidence of $\partial[\nu\partial^2 k/\partial x_i \partial x_i]/\partial t$ and $\partial\varepsilon/\partial t$ at the wall and it leads to

$$\frac{\partial \varepsilon}{\partial t} = \frac{\partial}{\partial t}\left[\nu \frac{\partial^2 k}{\partial x_i \partial x_i}\right] = -2\nu F_1 + 24\nu^2 E_1 \quad . \tag{31}$$

In the exact equations for k and ε, this coincidence condition is ensured by many additional correlation terms. Some of these terms are neglected in modeling, therefore, it is possible that the resultant k and ε are bound to each other in ways that are not found in the exact equations. Shima[12] proposes to partially compensate the effects of the neglected correlation terms by modeling the ε-equation so that the coincidence condition at the wall is satisfied. The result is an additional ξ term in the modelled ε-equation. This idea is adopted by SH and LS. The impact of this on the modelled results will be assessed in the next section when the channel flow calculations are discussed.

6. Comparisons with Plane Channel Flow Data

The near-wall closures examined above are used to close the mean flow equations (1) and (2) written in Cartesian coordinates for a fully-developed channel flow at a Re = 6500. Since the flow is fully-developed, the mean flow equations can be reduced to a single equation involving the mean velocity U and the Reynolds shear stress[15]. Thus, the problem is simplified to solving one mean flow, four Reynolds-stress and one dissipation-rate equations. These are ordinary differential equations, therefore, they can be solved by a known numerical method, such as the Newtonian iteration technique used in Refs. 11 and 15. This means that a common, well established numerical technique can be used to perform all calculations and the numerical errors involved will be the same for each model calculation. In other words, a true comparison of the performance of the near-wall closures can be made for this particular problem. Any discrepancies in the results could be attributed to model differences and not to numerical errors.

A fixed grid is maintained for all calculations. The grid distribution is such that there are five grid points in the region, $0 \le y^+ \le 5$, 15 grid points in the region, $15 \le y^+ \le 65$, and 31 grid points in the region, $65 \le y^+ \le Re_\tau$, where $Re_\tau = u_\tau H/\nu$ is the Reynolds number based on the friction velocity and 2H is the channel width. Since Re_τ is related to Re by $Re_\tau = (u_\tau/2U_o)Re$, where U_o is the centerline velocity, it serves as the only input paramenter to the problem subject to the following boundary conditions for U, the Reynolds stresses and ε. If the x-coordinate is aligned with the channel mid-plane, the boundary conditions at y = H can be written as,

$$U = \overline{u^2} = \overline{v^2} = \overline{w^2} = \overline{uv} = 0, \tag{32a}$$

$$\varepsilon = 2\nu(d\sqrt{k}/dy)^2, \tag{32b}$$

while the boundary conditions at y = 0 are given by,

$$d\varepsilon/dy = d\overline{u^2}/dy = d\overline{v^2}/dy = d\overline{w^2}/dy = 0 \text{ and } \overline{uv} = 0. \tag{33}$$

These boundary conditions are applicable for all closures except SY. In that case, (32a) and (33) apply but (32b) does not. The latter condition should be replaced by $\tilde{\varepsilon} = 0$, because the ε-equation solved in the SY closure is a modified form of Chien's equation[32], which is a transport equation for a pseudo dissipation rate.

Direct numerical simulation of the Navier-Stokes equations has also been used to solve the channel flow problem at the same Re[25,26]. Turbulence statistics of the calculated flow are reported in Ref. 25 while the Reynolds-stress and dissipation-rate budgets are given in Ref. 26. As a result, the near-wall asymptotic behavior of the Reynolds stresses can be determined from these results and their limiting values are found to be consistent with another set of experimental data[45], even though the two sets of data are obtained at different Re. In view of this, these two sets of data[25,26,45] are most appropriate for assessing the internal consistency of the limiting behavior of near-wall closures. Specifically, the modelled limiting behavior of the Reynolds stresses, such as that given in equation (8), is compared with the chosen data. In addition, from (8) and (11), it can be deduced that $k^+/\varepsilon^+y^{+2} = 0.5$ and $(a_u^2 + a_v^2 + a_w^2)/a_k = 2.0$. The ability of the near-wall closures to recover these limiting values is analysed. Finally, comparisons of the distributions of the Reynolds stresses across the channel and their near-wall budgets will also be presented. It is hoped that, through this rigorous comparison, the strengths and weaknesses of the various near-wall closures could be identified.

The simulated, measured and modelled limiting values at the wall are shown in Table 4. Since Nishino and Kasagi[45] did not report on any ε measurement, the limiting value k^+/ε^+y^{+2} could not be estimated. Furthermore, their value of $(a_u^2 + a_v^2 + a_w^2)/a_k$ is larger than 2.0. This means that their measurement of a_u is probably too large. Other than that, their measurements are very consistent with those of Ref. 25. It should be pointed out that only the modelled results of HL, PE, KLY, SY, SH, LSH and LS are given. In the SY calculation, HL72 and LRR1 are chosen as the models for the diffusion and pressure redistribution terms, respectively. The same

numerical technique is used to calculate the flow for each closure. However, after numerous attempts, convergent solutions for LT are not possible under the uniformly applied convergency criterion of normalized residual value less than 10^{-4} for all calculations. On the other hand, if the convergency criterion is relaxed, convergent solutions become possible. Since all comparisons are made on the same basis, the results of LT are not listed in Table 4.

Based on the near-wall analyses and the results listed in Table 3, it could be concluded that HL, PE and KLY could not perform well in their predictions of the limiting values at the wall because the 11, 22, 33 and 13 components of $(D^{v}_{ij} + \Phi^{p}_{ij} + \Phi_{ij} - \varepsilon_{ij})$ are not zero at the wall unless C_1 is set equal to one or the random functions a_i, b_i, and c_i are required to satisfy certain constraints. Indeed, this is the case as indicated by the calculated limiting values shown in Table 4 and the results are at variance with simulation data. First of all, the calculated normal stresses are fairly isotropic near the wall. This is evidence by the approximately equal values of a_u, a_v and a_w calculated by HL, PE and KLY. The calculated a_{uv} is several times larger than the data shown while the calculated a_k is several times smaller. Even though the limiting values for $(a_u^2 + a_v^2 + a_w^2)/a_k$ are approximately correct, the calculated values for k^+/ε^+y^{+2} are not. This means that the closures are not internally consistent and asymptotically incorrect. On the other hand, SY goes to zero at the wall for every component of $(D^{v}_{ij} + \Phi^{p}_{ij} + \Phi_{ij} - \varepsilon_{ij})$. However, this is achieved at the expense of solving a modified form of Chien's ε-equation[32] that does not satisfy the true boundary condition at the wall. Consequently, the limiting values calculated using this closure are all incorrect. This means that the ε-equation of Chien[32] is not at all suitable for near-wall turbulent flow calculations.

The other three closures, SH, LSH and LS, give very reasonable results compared to simulation data as well as measurements. This is a consequence of the fact that they are formulated to satisfy the asymptotic near-wall behavior of either the velocity-pressure-gradient correlation or the exact Reynolds-stress equations or both. The limiting values for $(a_u^2 + a_v^2 + a_w^2)/a_k$ are recovered exactly while the values for k^+/ε^+y^{+2} are correct to within 4%. There are two major

differences between these three closures though. One is in the predictions of a_u and a_k, while the other is in the calculations of a_v and a_{uv}. LSH gives a more correct predictions of a_u and a_k. However, its calculations of a_v and a_{uv} are greater than the data shown by approximately one order of magnitude. On the other hand, the reverse is true for SH and LS. There is one exception though, and that is the prediction of a_v by SH. Its value is as large as that calculated by LSH. The reason could be due to the fact that LS tries to match the asymptotic behavior to higher orders of y for the 12, 23 and 22 components of $(D^v_{ij} + \Phi^p_{ij} + \Phi_{ij} - \varepsilon_{ij})$. If the predictions of a_u and a_k are to be improved, one suggestion could be to try to match the 11 component of $(D^v_{ij} + \Phi^p_{ij} + \Phi_{ij} - \varepsilon_{ij})$ to y^2 in the near-wall region.

Another test of the internal consistency of the near-wall closures can be carried out by comparing the limiting values of the structure parameters, a_u^2/a_k, a_v^2/a_k, a_w^2/a_k and $a_{uv}/a_u a_v$, with data. These values are also listed in Table 4 for comparison. Both the direct simulation results and measurements give an a_v^2/a_k value that is closed to zero at the wall. On the other hand, the value of a_u^2/a_k is about 3.5 to 6 times that of a_w^2/a_k and $a_{uv}/a_u a_v = 0.22$ to 0.26, respectively. The measured ratio a_u^2/a_k is on the high side because of a probable incorrect measurement of a_u. None of the closures, HL, PE, KLY and SY, examined give limiting behavior of a_u^2/a_k, a_v^2/a_k and a_w^2/a_k that is even closed to the data, especially the calculated a_v^2/a_k, which is at least two orders of magnitude greater than the data shown. However, HL and PE give fairly accurate predictions of $a_{uv}/a_u a_v$. The calculated ratio of a_u^2/a_k over a_w^2/a_k from SH is approximately equal to the measured result but its calculated a_v^2/a_k is two orders of magnitude larger than the simulated value and its prediction of $a_{uv}/a_u a_v$ is abouit half that of the measurement. As for LSH, its predictions of the ratio a_u^2/a_k over a_w^2/a_k and $a_{uv}/a_u a_v$ are twice as large as the data. On the other hand, LS's prediction of a_v^2/a_k is much closer to that of the data but its calculation of $a_{uv}/a_u a_v$ is about the same as SH. It seems that SH and LS are the only closures that could replicate the limiting behavior approximately. Therefore, it could be concluded that, overall, three closures are capable of reproducing the near-wall behavior more correctly than other closures examined. Furthermore, they are internally more

consistent in terms of the predicted limiting values of the structure parameters, the Reynolds stresses and the dissipation rate.

The plots of $-\overline{uv}^+$, k^+, and the three normal stresses u^+_{rms}, v^+_{rms} and w^+_{rms} are shown in Figs. 1 - 3. In each plot, part (a) shows the near-wall distributions given in terms of the wall variable y^+, while part (b) displays the overall profiles in terms of the outer variable (1 - y/H). Each panel of each plot shows the comparison of the modelled calculation with direct simulation result[25]. The calculations are represented by solid curves, while the simulation results are denoted by dashed curves.

From these plots, it can be seen that LS gives the best overall prediction of $-\overline{uv}^+$ in both the near-wall and outer region. The maximum $-\overline{uv}^+$ is also calculated correctly (Fig. 1). The next best predictions are those given by LSH, KLY and HL. Here, the closures under-predict the maximum $-\overline{uv}^+$. The other closures, PE, SY and SH, on the other hand, give an incorrect prediction of the near-wall distribution of $-\overline{uv}^+$. In a fully-developed channel flow, the mean velocity only depends on the shear stress distribution across the channel. Therefore, if a closure under- or over-predicts the turbulent shear stress, its calculation of the mean velocity profile is more than likely to be incorrect also.

As far as k^+ is concerned, HL, PE and SY under-predict its value all across the channel, in the near-wall as well as in the outer region (Fig. 2). HL and PE even greatly under-predict the value of k^+ in the channel mid-plane. On the other hand, KLY over-predicts k^+ in the outer region but its prediction in the near-wall region is better than those of HL, PE and SY. The calculation of SH is, in general, slightly lowered than the simulation data. On the other hand, the near-wall prediction of k^+ by LSH agrees well with simulation data. However, it over-estimates the value of k^+ slightly in the outer region. Even though LS under-predicts the maximum k^+ just like LSH, it does give a fairly correct prediction of the k^+ profile across the channel. In general, the best overall predictions of k^+ are given by LSH and LS.

Finally, the same can also be said of the predictions of u^+_{rms}, v^+_{rms} and w^+_{rms} (Fig. 3). Only SH, LSH and LS could reproduce the anisotropic behavior of the normal stresses near the wall, the other closures invariably give a fairly isotropic prediction. Even though the normal stress predictions are fairly anisotropic for SH, its calculation of v^+_{rms} is substantially higher than data in the region $y^+ < 30$. This over-prediction of v^+_{rms} would lead to an incorrect calculation of the $-\overline{uv}$ budget and, thus, renders SH less attractive compared to LSH and LS. The major reason for the noted discrepancy lies in the modeling of the $(\Phi^p_{ij} + \Phi_{ij})$ term. SH, LSH and LS attempt to partially model Φ^p_{ij} in the near-wall region. In the process, they also try to partially compensate for the incorrect near-wall behavior of Φ_{ij}. Consequently, all components of $(D^\nu_{ij} + \Phi^p_{ij} + \Phi_{ij} - \varepsilon_{ij})$ vanish at the wall independent of the behavior of the random functions a_i, b_i and c_i.. This, however, is not true for HL, PE and KLY; therefore, it is not surprising that they fail to give the correct predictions of the normal stresses. Again, LSH slightly over-predicts the normal stresses in the outer region.

The plots of $\varepsilon H/u^3_\tau$ versus (1.0 - y/H) and $\varepsilon H/u^3_\tau$ versus y^+ are given in Fig. 4. Here, the comparisons are carried out to assess the performance of the different closures relative to each other. With the exception of SY, the general trend of the predicted ε is about the same. The behavior can be described by a general increase of ε towards the wall. Just before the wall, a maximum is reached and this is followed by a rapid drop to a finite wall value. This trend, in particular, the near-wall behavior, is contrary to simulation data[26], where ε increases to a maximum at the wall. Since all these closures satisfy the boundary condition that the wall ε^+ is equal to $2a_k$, the calculated behavior of ε in the near-wall region could not be due to an incorrect specification of the boundary condition. Rather, it is the consequence of inappropriate near-wall models for either the Reynolds-stress equations or the ε-equation. However, judging from other predicted quantities, this incorrect behavior of ε in the near-wall region does not seem to have a significant effect on the calculations of the Reynolds stresses and structure parameters, especially in the case of LS, LSH and SH.

From the above comparisons, it is clear that HL, PE, KLY and SY perform poorly as near-wall closures. Therefore, their predictions of the Reynolds-stress and k budgets would also be incorrect. On the other hand, the budgets deduced from SH and LSH with the exception of the $-\overline{uv}$ budget are very similar while those of LS have been presented in Ref. 15. In view of this, only the budget plots of LSH and HL for $\overline{u^2}$, k and $-\overline{uv}$ are shown for comparison with simulation data in Figs. 5 - 7. The sample plots presented here together with those given in Ref. 15 serve to illustrate the discrepancies between closure calculations and data. It is hoped that, through this evaluation, an approach to improve the closures could be identified.

All budget plots shown in Figs. 5 - 7 and those presented in Ref. 15 give an incorrect prediction of ε_{11}, ε_{12} and ε, especially in the region, $0 \leq y^+ \leq 20$. According to simulation results, the absolute maximum of ε_{11} and ε occurs at the wall. The model calculations, on the other hand, show that their absolute maximum appears away from the wall. There is, of course, a drop from these maxima to some finite wall values. Since viscous dissipation is balanced exactly by viscous diffusion at the wall, it follows that the calculated wall values of the viscous diffusion of $\overline{u^2}$ and k are also incorrect, in spite of the fact that their predicted trends are similar to those of simulation data (Figs. 5 and 6). In LSH's calculation of the $\overline{u^2}$ budget, viscous diffusion is balanced by both dissipation and velocity-pressure-gradient correlation (Fig. 5). This is a consequence of the incorrect modeling of the velocity-pressure-gradient term. In general, all closures give a poor prediction of the behavior of the velocity-pressure-gradient correlation term in the near-wall region; in particular, the behavior in the 12 component (Fig. 7). This is especially true of HL where the calculated value is about four times larger than data. The reason is because $\overline{v^2}$ is responsible for production in the $-\overline{uv}$ equation and HL gives a substantially higher prediction of this nomal stress in the near-wall region (see Fig. 3a). Since production of $-\overline{uv}$ has to be balanced by the velocity-pressure-gradient correlation of $-\overline{uv}$, the result is a totally incorrect prediction of this budget. Consequently, the $-\overline{uv}$ budget obtained from HL is shown in Fig. 7 with a scale different from

that of LSH and simulation data. This is another indication that HL is not an asymptotically correct near-wall closure.

The wall values of ε_{12}, ε_{22} and ε_{33} are zero and hence the viscous diffusion is also zero for these components. Even though these calculated trends are consistent with simulation data, the magnitudes of the calculated distributions of the viscous diffusion along the 12, 22 and 33 components are several times larger than the simulated values. This evaluation, therefore, reveals that although SH, LSH and LS give good predictions of the turbulence statistics, their calculations of the Reynolds-stress and k budgets are still not quite correct.

There are many reasons for this incorrect prediction. However, the two most important factors could be the ε-equation and the modeling of the velocity-pressure-gradient term in the near-wall region. Lai and So[15] did a preliminary investigation to show that the correct behavior of ε_{11} and ε could be achieved by modifying the ε-equation. Unfortunately, the modification also affects the calculation of other statistical properties. As a result, the overall predictions are not as satisfactory as before. In spite of this rather inconclusive result, their study did manage to show that, perhaps, the ε-equation could be properly modified to remedy the incorrect prediction of ε_{11} and ε. This approach has been adopted by So et al.[56] and they manage to successfully modify the ε-equation to give a correct prediction of the turbulence statistics and the behavior of ε in a flat plate boundary-layer flow. Further comments about the ε-equation of So et al.[56] and its performance in terms of the prediction of the channel flow problem are given in the next section.

7. Proposed Improvement

The above analysis reveals that, among the eight closures examined, three manage to give the best overall predictions of the turbulence statistics in a fully-developed channel flow. However, not a single closure can reproduce the near-wall distributions of ε_{11} and ε correctly. Even SH, LSH and LS can only correctly replicate ε_{11} and ε up to $y^+ \approx 20$. Thereafter, their predictions of ε_{11} and ε are totally incorrect. Lai and So[15] argued that the inability of their closure to predict the near-wall distributions of ε_{11} and ε lies in the incorrect modeling of the near-wall production and dissipation terms proposed for the ε-equation as well as in the near-wall modeling of the velocity-pressure-gradient correlation. Since the modeling of the ε-equation is rather ad hoc, a first attempt to improve these predictions could be achieved by modifying the near-wall production and dissipation terms proposed for the ε-equation. A preliminary effort has been made by So et al.[56] They used the ε-equation of Ref. 15 as a base and suggested an alternative ξ function based on the studies of Shima[12] and Mansour et al.[55] The proposed ξ is given by

$$\xi = f_{w,2}\left[-2\frac{\varepsilon\tilde{\varepsilon}}{k} + 3\frac{\varepsilon^{*2}}{2k}\right] \quad . \tag{34}$$

In modifying the ε-equation, So et al.[56] maintained the values of most model constants specified in LS but found that they have to change $C_{\varepsilon 1}$ to 1.50 and the definition of σ to $[1 - 1.5\exp(-Re/10^4)]$. Thus modified, the ε-equation is incorporated into a k-ε closure to calculate flat plate boundary-layer flows. Their results show that the calculated properties are in very good agreement with measurements and that the limiting values of the structure parameters and the near-wall ε distribution behave similarly to the direct simulation result of a flat plate boundary layer[27].

In order to verify that the primary cause for the incorrect ε_{11} and ε behavior near a wall is the ε-equation, it is suggested to improve one of the near-wall closures identified above by adopting the modified ε-equation of So et al.[56] Such an improved near-wall closure could be

obtained from the Reynolds-stress models of Refs.12, 14 or 15 and the ε-equation of Ref. 56. Here, the example is carried out with the models of Ref. 15. The resultant closure, designated as LSZS, is used to calculate the fully-developed channel flow considered above and the calculated limiting values of the Reynolds stresses and structure parameters are listed in Table 4 for comparison. Furthermore, the plots of the Reynolds stresses, k and ε are shown in Figs. 1 - 4. Near-wall budgets of $\overline{u^2}$, $-\overline{uv}$ and k are plotted in Figs. 5 - 7. It can be seen that LSZS gives the best overall prediction of the limiting values of the Reynolds stresses and structure parameters (see Table 4). Most important of all, the calculated a_k agrees to within 4% of the simulated data. This means that, for the first time, the wall ε^+ is predicted correctly. In addition, the calculated a_u and a_w are in very good agreement with data compared to other closures, including LSH. As a result, the calculated structure parameters are also in better agreement with data.

A comparison of the distributions of the Reynolds stresses, k and ε reveals that LSZS gives better predictions of the overall profiles, including the near-wall behavior of ε (Figs. 1 - 4). In spite of the good agreement shown, two slight discrepancies should be noted. One is in the near-wall prediction of the distribution of $-\overline{uv}$, while another is in the calculation of k near the channel center. LSZS over-predicts $-\overline{uv}$ in the near-wall region and is a conseqence of the incorrect prediction of a_{uv}, which is probably due to an incomplete modeling of the pressure diffusion term near the wall. It also under-predicts k near the channel center and is primarily caused by an under-estimation of $\overline{v^2}$ in the outer region of the channel. This under-estimation, however, is most likely tied to the model for pressure redistribution. Therefore, the calculated results could be further improved by modifying these two models.

For the first time, the near-wall behavior of ε_{11} and ε is predicted correctly in a qualitative sense (Figs. 5 and 6). The calculated distributions do not show a distinct plateau in the region, $8 < y^+ < 15$, compared to those given by direct simulation. However, they do increase to a maximum at the wall. The calculated wall values of $-\varepsilon_{11}$ and $-\varepsilon$ are -0.28 and -0.172, respectively, and they compare favorably with the simulated values of approximately -0.26 and -0.166. Consequently,

the wall values of viscous diffusion for the $\overline{u^2}$ and k components are also predicted correctly, and so is the steep rise of the viscous diffusion term in the near-wall region. Even though the modification improves the prediction of the budgets of $\overline{u^2}$ and k, it has very little effect on the $-\overline{uv}$ budget (Fig. 7). Again, the calculated $-\varepsilon_{12}$ is 2 to 3 times larger than the simulated value and is in close agreement with that predicted by LS. As for the budgets of $\overline{v^2}$ and $\overline{w^2}$, they are essentially identical to those of LS and, therefore, the predictions of ε_{22} and ε_{33} are again several times larger than the simulated values. In view of this, the improvement fails to completely remedy all the discrepancies noted in Section VI.

From the above comparisons, it can be seen that the improvement made to the ε-equation does not significantly alter the calculated turbulence statistics (Figs. 1 - 4) and the various terms in the Reynolds-stress and k budgets (Figs. 5 - 7). It only changes the distributions of ε_{11} and ε near the wall (Figs. 5 and 6). This means that the behavior of ε_{11} and ε is very much influenced by the modelled ε-equation and substantiates the approach taken by So et al.[56] to improve near-wall closures. Therefore, this analysis suggests that further improvement to second-order near-wall turbulence closures is still needed and this could be achieved by modifying the models proposed for the velocity-pressure-gradient correlation term. It is hoped that, through this further improvement, the behavior of ε_{12}, ε_{22} and ε_{33}, the near-wall distribution of $-\overline{uv}$ and the centerline value of k could be predicted satisfactorily.

Based on the above improvement, it is now possible to calculate the turbulence statistics of a fully-developed channel flow fairly correctly using a second-order near-wall turbulence closure. Also, for the first time, the behavior of ε_{11} and ε in the near-wall region has been calculated correctly. However, improvements are still needed to remedy the discrepancies noted in the predictions of ε_{12}, ε_{22}, ε_{33} and $-\overline{uv}$ in the near-wall region and the calculation of k near the centerline.

8. Concluding Remarks

A total of eight near-wall Reynolds-stress closures has been reviewed. All closures examined essentially adopt the same high-Reynolds-number models for turbulent diffusion, dissipation and pressure redistribution. Invariably the pressure diffusion part of the velocity-pressure-gradient correlation is neglected in all high-Reynolds-number closures. Different approaches have been proposed to modify these closures for near-wall flows. Some adopt the philosophy that only the model for dissipation needs modification, while others argue for modifications of the models for both dissipation and pressure redistribution. Some others also argue for the inclusion of pressure diffusion effects in the near-wall region; therefore, suggesting that the velocity-pressure-gradient correlation has to be modelled in the near-wall region rather than pressure redistribution alone. All modifications are proposed so that the resultant closure satisfied the constraints imposed by the near-wall asymptotic behavior of the Reynolds stresses. With the exception of SY, all closures examined solved a transport equation for the true dissipation rate of the turbulent kinetic energy. On the other hand, SY solves a pseudo dissipation-rate equation that satisfies a homogeneous wall boundary condition. These dissipation-rate equations are further modified to mimick the exact near-wall behavior. As a result, a uniform claim of all these closures is that they are asymptotically correct as a wall is approached.

The modelled equations are examined for their asymptotic behavior near a wall and the results are compared with the behavior deduced from the exact Reynolds-stress equations. Among the closures examined, it is found that four of them (HL, PE, KLY and LT) fail to go to zero at the wall for the 11, 22, 33 and 13 components of the equations without imposing some kind of constraints on C_1 or on the behavior of the random functions a_i, b_i and c_i. The others approach zero at the wall independent of the behavior of the random functions; however, their asymptotic behavior is not consistent with that required by the exact equations. LS matches the behavior to a higher order of y than SY, SH and LSH for the 12, 23 and 22 components (see Table 3), while the

behavior of the 11, 33 and 13 components is similar to that of SY, SH and LSH. A further check on the internal consistency of the closures is carried out by using them to calculate a fully-developed flow in a two-dimensional channel at a Re = 6500. These results are then compared with direct simulation and experimental data[25,26,45]. Specifically, the limiting values of the Reynolds stresses, the structure parameters and the dissipation rate are assessed. A common numerical technique is used to perform the calculation for each closure and a uniform convergency criterion is imposed on all calculations. Under these conditions, LT fails to give convergent solutions to the governing equations. Of the remaining seven calculations, it is found that four closures (HL, PE, KLY and SY) fail to give limiting values that approximate the simulation and experimental data examined. Their failure is most pronounced in the prediction of the turbulent stress normal to the wall and the shear stress. For example, the data examined shows that a_v^2/a_k goes to zero at the wall, while the closure calculations of HL, PE, KLY and SY give finite values that are comparable to the other structure parameters at the wall. On the other hand, SH, LSH and LS give internally consistent results that are asymptotically more correct compared to other closure calculations. However, one drawback of LSH is its calculation of a_v^2/a_k, which is still one order of magnitude larger than that obtained from LS, while the values of a_u and a_k deduced from SH and LS are quite a bit less than those of the simulated values. Therefore, SH, LSH and LS have their defects and should be further improved.

A comparison of the closure calculations with data further reveal that, with the exception of LSH and LS, all closures examined either over- or under-predict the turbulent shear stress in the near-wall region or under-predict the maximum shear. This means that they are more than likely to give an incorrect calculation of the mean velocity for the channel flow considered. Even though LS under-predicts the maximum turbulent kinetic energy, its overall prediction of the k profile is in good agreement with data. On the other hand, SH under-predicts k across the whole channel while LSH over-predicts k in the outer region. The other closures essentially give an incorrect prediction of k across the channel. Finally, only SH, LSH and LS are capable of reproducing the anisotropic

behavior of the normal stresses near the wall, while the other closures give a fairly isotropic near-wall behavior. Even then, SH's prediction of $\overline{v^2}$ in the near-wall region is about twice as large as the simulation data. Consequently, its calculation of the $-\overline{uv}$ budget is greatly in error. The reason is traced to the imbalance of the modelled equations in the near-wall region. In spite of these good comparisons by SH, LSH and LS, their calculations of ε_{11} and ε in the near-wall region are totally incorrect. The three closures give a maximum ε_{11} and ε away from the wall and a rapid drop to a finite value at the wall. On the other hand, simulation data shows that ε_{11} and ε reach their maximum value at the wall. As a result, the wall values of ε_{11}, ε and the viscous diffusion of $\overline{u^2}$ and k are greatly under-predicted.

A conjecture is then made that the incorrect prediction of ε_{11} and ε could be remedied by improving the near-wall behavior of the ε-equation. This conjecture is essentially verified by the calculations of LSZS . The LSZS closure is made up of the Reynolds-stress models of Ref. 15 and the ε-equation of Ref. 56. With this improvement, the calculated results are in much better agreement with data, including the near-wall distributions of ε_{11} and ε. The calculated limiting values of the Reynolds stresses give the best overall agreement with data, and so are the structure parameters. Also, for the first time, the wall values of ε_{11} and ε are replicated by LSZS. This means that the wall values of the viscous diffusion of $\overline{u^2}$ and k are also calculated correctly. However, some slight discrepancies exist in the predictions of ε_{12}, ε_{22}, ε_{33} and $-\overline{uv}$ in the near-wall region and k near the channel center. These discrepancies are relatively less important in the overall comparison. They could be attributed to an incorrect modeling of the velocity-pressure-gradient correlation near the wall and pressure redistribution near the channel center. Therefore, further improvements are required if a complete replication of the simulation data by a statistical model of turbulence is desirable.

References

[1]Schlichting, H., Boundary Layer Theory, McGraw Hill, New York, 4th edition, 1960, pp. 477-480.

[2]Kline, S.J., Cantwell, B.J. and Lilley, G.M.(eds), *Proc. 1980-81 AFOSR - HTTM - Stanford Conference on Complex Turbulent Flows,* Department of Mechanical Engineering, Stanford University, Stanford, CA 94035.

[3]Patel, V.C., Rodi, W. and Scheuerer, G., "Turbulence Models for Near-Wall and Low-Reynolds Number Flows: A Review, " *AIAA Journal,* **Vol. 23**, 1985, pp. 1308-1319.

[4]Launder, B.E., "Second-Moment Closure: Present ... and Future," *International Journal of Heat and Fluid Flow,* **Vol. 10**, 1989, pp. 282-300.

[5]Azzola, J., Humphrey, J.A.C., Iacovides, H. and Launder, B.E., "Developing Turbulent Flow in a U-Bend of Circular Cross-Section; Measurement and Computation," *Journal of Fluids Engineering,* **Vol 108**, 1986, pp. 214-221.

[6]Lai, Y. G., "Near-Wall Modeling of Complex Turbulent Flows," Ph.D. thesis, Mechanical and Aerospace Engineering, Arizona State University, Tempe, Arizona, 1990.

[7]Shih, T-H. and Lumley, J. L., "Second-Order Modeling of Near-Wall Turbulence," *Physics of Fluids,* Vol. **29**, 1986, pp. 971-975.

[8]Hanjalic, K. and Launder, B.E., "Contribution Towards a Reynolds-Stress Closure for Low-Reynolds-Number Turbulence," *Journal of Fluid Mechanics,* **Vol. 74**, 1976, pp. 593-610.

[9]Prud'homme, M. and Elghobashi, S., "Prediction of Wall-Bounded Turbulent Flows with an Improved Version of a Reynolds-Stress Model," *Proceedings, 4th Symposium on Turbulent Shear Flows,* Karlsruhe, West Germany, 1983, pp. 1-7-1-12.

[10]Kebede, W., Launder, B.E. and Younis, B.A., "Large Amplitude Periodic Pipe Flow: A Second Moment Closure Study," *Proceedings, 5th Symposium on Turbulent Shear Flows,* Ithaca, NY 1985, pp. 16-23 - 16-29.

[11]So, R.M.C. and Yoo, G.J., "On the Modeling of Low-Reynolds-Number Turbulence," *NASA CR-3994*, 1986.

[12]Shima, N.,"A Reynolds-Stress Model for Near-Wall and Low-Reynolds-Number Regions," *Journal of Fluids Engineering,* **Vol. 110**, 1988, pp. 38-44.

[13]Launder, B.E. and Tselepidakis, D.P., "Contribution to the Second-Moment Modeling of Sublayer Turbulent Transport," *Zaric Memorial International Seminar on Near-Wall Turbulence*, Yugoslavia, May 16-20, 1988.

[14]Launder, B.E. and Shima, N., "Second-Moment Closure for the Near-Wall Sublayer: Development and Application," *AIAA Journal*, **Vol. 27**, 1989, pp. 1319-1325.

[15]Lai, Y.G. and So, R.M.C., "On Near-Wall Turbulent Flow Modeling," *Journal of Fluid Mechanics*, **Vol. 221**, 1991, pp. 641-673.

[16]Prud'homme, M. and Elghobashi, S., "Turbulent Heat Transfer Near the Reattachment of Flow Downstream of a Sudden Pipe Expansion," *Numerical Heat Transfer*, **Vol. 10**, 1986, pp. 349-368.

[17]So, R.M.C. and Yoo, G.J., "Low-Reynolds-Number Modeling of Turbulent Flows With and Without Wall Transpiration," *AIAA Journal*, **Vol. 25**, 1987, pp. 1556-1564.

[18]So, R.M.C., Lai, Y.G., Hwang, B.C. and Yoo, G.J., "Low-Reynolds-Number Modeling of Flows Over a Backward-Facing Step," *Zeitschrift für angewandte Mathematik und Physik*, **Vol. 39**, 1988, pp. 13-27.

[19]Yoo, G.J. and So, R.M.C., "Variable Density Effects on Axisymmetric Sudden-Expansion Flows," *International Journal of Heat and Mass Transfer*, **Vol. 32**, 1989, pp. 105-120.

[20]Pollard, A. and Martinuzzi, R., "Comparative Study of Turbulence Models in Predicting Turbulent Pipe Flow. Part II: Reynold Stress and k - ε Models," *AIAA Journal*, **Vol. 27**, 1989, pp. 1714-1721.

[21]Yoo, G.J., So, R.M.C. and Hwang, B.C., "Calculation of Developing Turbulent Flows in a Rotating Pipe," *Journal of Turbomachinery*, **Vol. 113**, 1991, pp. 34-41.

[22]Lai, Y.G. and So, R.M.C., "Near-Wall Modeling of Turbulent Heat Fluxes," *International Journal of Heat and Mass Transfer*, **Vol. 33**, 1990, pp. 1429-1440.

[23]So, R.M.C., Lai, Y.G. and Hwang, B.C., "Near-Wall Turbulence Closure for Curved Flows," *AIAA Journal*, **Vol. 29**, 1991.

[24]Moser, R.D. and Moin, P., "The Effects of Curvature in Wall-Bounded Turbulent Flow," *Journal of Fluid Mechanics*, **Vol. 175**, 1987, pp. 479-510.

[25]Kim, J., Moin, P. and Moser, R.D., "Turbulence Statistics in Fully Developed Channel Flow at Low Reynolds Number," *Journal of Fluid Mechanics*, **Vol. 177**, 1987, pp. 133-186.

[26]Mansour, N.N., Kim, J. and Moin, P., "Reynolds-Stress and Dissipation-Rate Budgets in a Turbulent Channel Flow," *Journal of Fluid Mechanics*, **Vol. 192**, 1988, pp. 15-44.

[27]Spalart, P.R., "Direct Simulation of a Turbulent Boundary Layer up to $R_\theta = 1410$," *Journal of Fluid Mechanics*, **Vol. 187**, 1988, pp. 61-98.

[28]Kim, J., "On the Structure of Pressure Fluctuations in Simulated Turbulent Channel Flow," *Journal of Fluid Mechanics*, **Vol. 205**, 1989, pp. 421-451.

[29]Kim, J. and Lee, M.J., "The Structure of Pressure Fluctuations in Turbulent Shear Flows," *Turbulent Shear Flows 7*, 1990, pp.

[30]Hanjalic, K. and Launder, B.E., "A Reynolds-Stress Model of Turbulence and Its Application to Thin Shear Flows," *Journal of Fluid Mechanics*, **Vol. 52**, 1972, pp. 609-638.

[31]Launder, B.E., Reece, G.J. and Rodi, W., "Progress in the Development of a Reynolds-Stress Turbulence Closure," *Journal of Fluid Mechanics*, **Vol. 68**, 1975, pp. 537-566.

[32]Chien, K.Y., "Predictions of Channel and Boundary Layer Flows with a Low-Reynolds-Number Two-Equation Model of Turbulence," *AIAA Journal*, **Vol. 20**, 1982, pp. 33-38.

[33]Kolmogorov, A.N., "Local Structure of Turbulence in Incompressible Viscous Fluid for Very Large Reynolds Number," *Doklady AN SSSR*, **Vol. 30**, 1941, pp. 299-303.

[34]Rotta, J.C., "Statistiche Theorie Nichthomogener Turbulenz,"*Zeitschrift für Physik*, **Vol. 129**, 1951, pp. 547-572; also **Vol. 131**, 1951, pp. 51-77.

[35]Shir, C.C., "A Preliminary Numerical Study of Atmospheric Turbulent Flows in the Idealized Planetary Boundary Layer," *Journal of Atmospheric Sciences*, **Vol. 30**, 1973, pp. 1327-1339.

[36]Daly, B.J. and Harlow, F.H., "Transport Equations in Turbulence," *The Physics of Fluids, Vol. 13*, 1970, pp. 2634 - 2649.

[37]Cormack, D.E., Leal, L.G. and Seinfeld, J.H., "An Evaluation of Mean Reynolds Stress Turbulence Models: The Triple Velocity Correlation," *Journal of Fluids Engineering*, **Vol. 100**, 1978, pp. 47-54.

[38]Amano, R.S. and Goel, P., "Investigation of Third-Order Closure Model of Turbulence for the Computation of Incompressible Flows in a Channel with a Backward-Facing Step," *Journal of Fluids Engineering*, **Vol. 109**, 1987, pp. 424-428.

[39]Lumley, J.L., "Computational Modeling of Turbulent Flows," *Advances in Applied Mechanics*, **Vol. 18**, 1978, pp. 123-1796.

[40]Eckelmann, H., "The Structure of The Viscous Sublayer and the Adjacent Wall Region in a Turbulent Channel Flow," *Journal of Fluid Mechanics*, **Vol. 65**, 1974, pp. 439-459.

[41]Schildknecht, M., Miller, J.A. and Meier, G.E.A., "The Influence of Suction on the Structure of Turbulence in Fully-Developed Pipe Flow," *Journal of Fluid Mechanics*, **Vol. 90**, 1979, pp. 67-107.

[42]Kreplin, H.P. and Eckelmann, H., "Behavior of the Three Fluctuating Velocity Components in the Wall Region of a Turbulent Channel Flow," *The Physics of Fluids*, **Vol. 22**, 1979, pp. 1233-1239.

[43]El Telbany, M.M.M. and Reynolds, A.J., "Turbulence in Plane Channel Flows," *Journal of Fluid Mechanics*, **Vol 111**, 1981, pp. 283-318.

[44]Alfredsson, P.H., Johansson, A.V., Haritonidis, J.H. and Eckelmann, H., "The Fluctuating Wall-Shear Stress and the Velocity Field in the Viscous Sublayer," *The Physics of Fluids*, **Vol. 31**, 1988, pp. 1026-1033.

[45]Nishino, K. and Kasagi, N., "Turbulence Statistics Measurements in a Two-Dimensional Channel Flow Using a Three-Dimensional Particle Tracking Velocimeter," *Proceedings, 7th Symposium on Turbulent Shear Flows*, Stanford, California, 1989, pp. 22-1.1 - 22-1.6.

[46]Laufer, J., "The Structure of Turbulence in Fully-Developed Pipe Flow," *NACA Report No. 1174*, 1954.

[47]Morrison, W.R.B. and Kronauer, R.E.,"Structural Similarity for Fully Developed Turbulence in Smooth Tubes," *Journal of Fluid Mechanics*, **Vol. 39**, 1969, pp. 117-141.

[48]Klebanoff, P.S., "Characteristics of Turbulence in a Boundary Layer with Zero Pressure Gradient," *NACA Technical Note 1247*, 1955.

[49]Kasagi, N., Hirata, M. and Nishino, K., "Streamwise Pseudo-Vortical Structures and Associated Vorticity in the Near-Wall Region of a Wall-Bounded Turbulent Shear Flow," *Experiments in Fluids*, **Vol. 4**, 1986, pp. 605-614.

[50]Sirkar, K. and Hanratty, T.J., "The Limiting Behavior of the Turbulent Transverse Velocity Component Close to a Wall," *Journal of Fluid Mechanics*, **Vol. 44**, 1970, pp. 605-614.

[51]Derksen, R.W. and Azad, R.S., "Behavior of the Turbulent Energy Equation at a Fixed Boundary," *AIAA Journal* , **Vol. 19**, 1981, pp. 238-239.

[52]Jones, W.P. and Launder, B.E., "The Prediction of Laminarization with a Two-Equation Model of Turbulence," *International Journal of Heat and Mass Transfer*, **Vol. 15**, 1972, pp. 301-314.

[53]Launder, B.E. and Reynolds, W.C., "Asymptotic Near-Wall Stress Dissipation Rates in a Turbulent Flow," *The Physics of Fluids*, **Vol. 26**, 1983, pp. 1157-1158.

[54]Lumley, J.L., "Second-Order Modeling of Turbulent Flows," Prediction Methods for Turbulent Flows, Kollmann, W. (ed), Hemisphere, New York, 1980, pp. 1-31.

[55]Mansour, N.N., Kim, J, and Moin, P., "Near-Wall k-ε Turbulence Modeling," *AIAA Journal*, **Vol. 27**, 1989, pp. 1068-1073.

[56]So, R.M.C., Zhang, H.S. and Speziale, C.G., "Near-Wall Modeling of the Dissipation-Rate Equation," *AIAA Journal*, **Vol. 30**, 1992.

Table 1. Summary of high-Reynolds-number models for D_{ij}^{T}, Φ_{ij} and ε_{ij}.

Closure Source	D_{ij}^{T}	Φ_{ij}	ε_{ij}
Hanjalic and Launder (HL)[8]	HL72	LRR1	KV
Prud'homme and Elghobashi (PE)[9]	DH	LRR1	KV
Kebede, Launder and Younis (KLY)[10]	DH	LRR2	KV
So and Yoo (SY)[11]	HL72, SR	RA, LRR1, LRR2	KV
Shima (SH)[12]	HL72	LRR1	KV
Launder and Tselepidakis (TL)[13]	DH	modified LRR	KV
Launder and Shima (LSH)[14]	DH	LRR2	KV
Lai and So (LS)[15]	HL72	LRR1	KV

Table 2. Summary of near-wall turbulence properties.

Source	Re x 10^{-4}	a_u	a_v	a_w	a_k	a_{uv}	$(u^+_{rms})_m$ $(y^+)_m$	$(v^+_{rms})_m$ $(y^+)_m$	$(w^+_{rms})_m$ $(y^+)_m$	$(k^+)_m$ $(y^+)_m$	$(\overline{-u^+v^+})_m$ $(y^+)_m$
Kim, Moin & Moser[25]	0.65	0.36	0.009	0.19	0.0829	0.00072	2.656 (14)	0.844 (50)	1.094 (40)		0.725 (30)
Kreplin & Eckelmann[42]	0.77	0.25		0.065	0.035		2.85 (13)	1.0 (40)	1.2 (20)		
El Telbany & Reynolds[43]	6.46	0.28	0.005	0.08			2.8 (18)				
Alfredsson et al.[44]	0.76	0.40		0.20			2.924 (15)				
Nishino & Kasagi[45]	0.751	0.45	0.00735	0.18	0.11	0.00085	2.731 (13)	0.885 (50)	1.154 (40)	4.308 (15)	0.697 (30)
Laufer[46]	5.0	0.31	0.007	0.08		0.0008	2.65 (17)	0.925 (75)	1.30 (70)		0.889 (50)
Morrison & Kronauer[47]	3.4	0.40					3.02 (15)				
Klebanoff[48]	0.75*	0.31					3.05 (19)				

* Based on boundary layer momentum thickness

Table 3. Lowest order term in $(D_{ij}^{\nu} + \Phi_{ij}^{p} + \Phi_{ij} - \varepsilon_{ij})$.

Closure	Componets of $(D_{ij}^{\nu} + \Phi_{ij}^{p} + \Phi_{ij} - \varepsilon_{ij})$					
	11	33	13	12	23	22
Exact Eq. (3)	$O(y^3)$	$O(y^3)$	$O(y^3)$	$O(y^4)$	$O(y^4)$	$O(y^5)$
HL[8]	$-2\nu C_1\left(\overline{a_1^2} - \frac{A}{3}\right) + O(y)$	$-2\nu C_1\left(\overline{c_1^2} - \frac{A}{3}\right) + O(y)$	$-2\nu C_1\,\overline{a_1 c_1} + O(y)$	$O(y)$	$O(y)$	$2\nu C_1\, A/3 + O(y)$
PE[9]	$(1 - C_1)2\nu\left(\overline{a_1^2} - \frac{A}{3}\right) + O(y)$	$(1 - C_1)2\nu\left(\overline{c_1^2} - \frac{A}{3}\right) + O(y)$	$- C_1 2\nu\overline{a_1 c_1} + O(y)$	$O(y)$	$O(y)$	$(C_1 - 1)\, 2\nu A/3 + O(y)$
KLY[10]	$-C_1 2\nu\left(\overline{a_1^2} - \frac{A}{3}\right) + O(y)$	$-C_1 2\nu\left(\overline{c_1^2} - \frac{A}{3}\right) + O(y)$	$-C_1 2\nu\,\overline{a_1 c_1} + O(y)$	$O(y)$	$O(y)$	$C_1\, 2\nu\, A/3 + O(y)$
SY[11]	$O(y)$	$O(y)$	$O(y)$	$O(y)$	$O(y)$	$O(y^2)$
SH[12]	$O(y)$	$O(y)$	$O(y)$	$O(y)$	$O(y)$	$O(y^2)$
LT[13]	Finite	Finite	Finite	$O(y)$	$O(y)$	Finite
LSH[14]	$O(y)$	$O(y)$	$O(y)$	$O(y)$	$O(y)$	$O(y^2)$
LS[15]	$O(y)$	$O(y)$	$O(y)$	$O(y^2)$	$O(y^2)$	$O(y^3)$

Table 4. Simulated, measured and modelled asymptotic behavior at the wall

Source	$Re(10^{-4})$	a_u	$a_v(10^2)$	a_w	$a_{uv}(10^3)$	$a_k(10^2)$	k^+/ε^+y^{+2}	$\frac{a_u^2 + a_v^2 + a_w^2}{a_k}$	$\frac{a_u^2}{a_k}$	$\frac{a_v^2}{a_k}$	$\frac{a_w^2}{a_k}$	$\frac{a_{uv}}{a_u a_v}$
Nishino and Kasagi[45]	o.751	0.45	0.735	0.18	0.85	11.00	----	2.14	1.841	0.0005	0.295	0.26
Kim, Moin and Moser[25]	0.65	0.36	0.90	0.19	0.72	8.29	0.50	2.00	1.563	0.001	0.436	0.22
HL[8]	0.65	0.108	10.33	0.104	2.00	1.65	0.41	2.01	0.707	0.647	0.656	0.18
PE[9]	0.65	0.117	12.58	0.105	3.20	1.95	0.38	2.09	0.702	0.812	0.566	0.22
KLY[10]	0.65	0.147	10.35	0.138	1.90	2.58	0.45	1.99	0.838	0.415	0.738	0.12
SY[11]	0.65	0.174	13.60	0.138	11.60	3.18	----	2.14	0.952	0.582	0.599	0.49
SH[12]	0.65	0.212	5.43	0.089	1.50	2.79	0.50	2.00	1.606	0.106	0.285	0.13
LSH[14]	0.65	0.312	4.14	0.089	6.10	5.36	0.48	2.00	1.817	0.032	0.149	0.47
LS[15]	0.65	0.242	0.78	0.110	0.20	3.53	0.48	2.00	1.659	0.0017	0.343	0.11
LSZS	0.65	0.380	2.08	0.177	1.40	8.80	0.50	2.00	1.642	0.0049	0.358	0.18

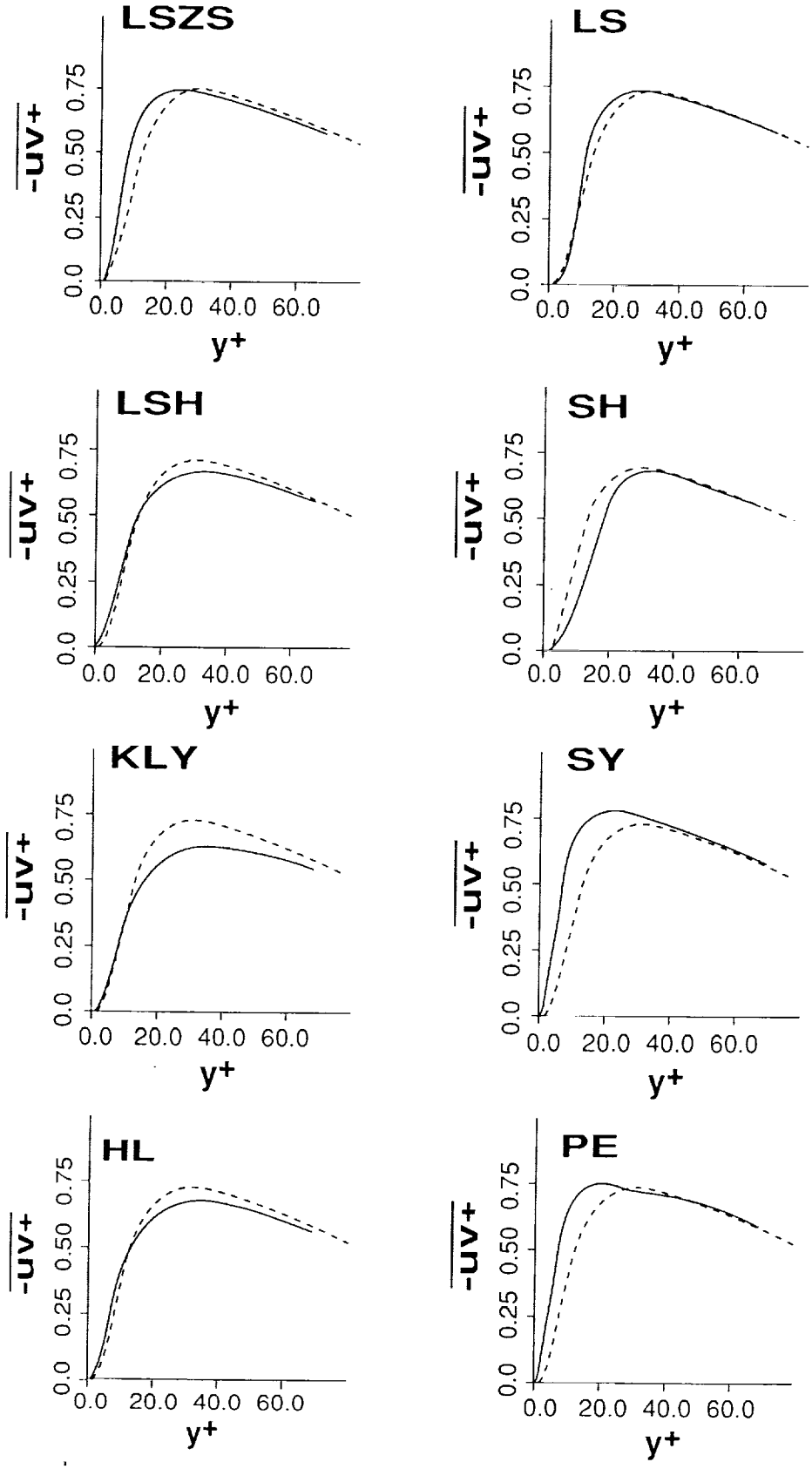

Figure 1a. Distributions of $-\overline{uv}^+$ in a fully-developed channel flow: ___ model calculation; ----, direct simulation data[25]; near-wall behavior.

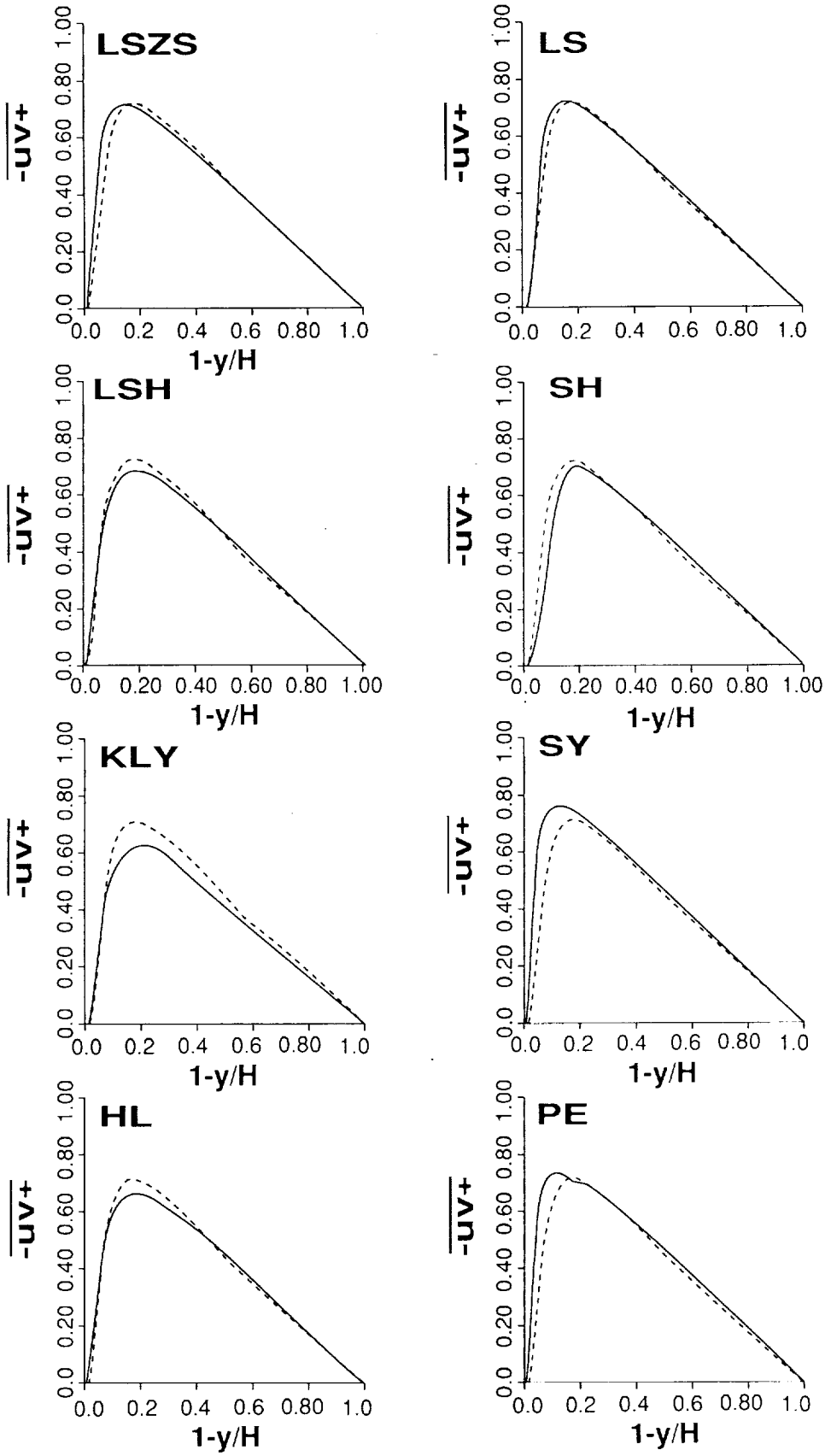

Figure 1b Distributions of $-\overline{uv}^+$ in a fully-developed channel flow: ___ model calculation; ----, direct simulation data[25]; outer flow behavior.

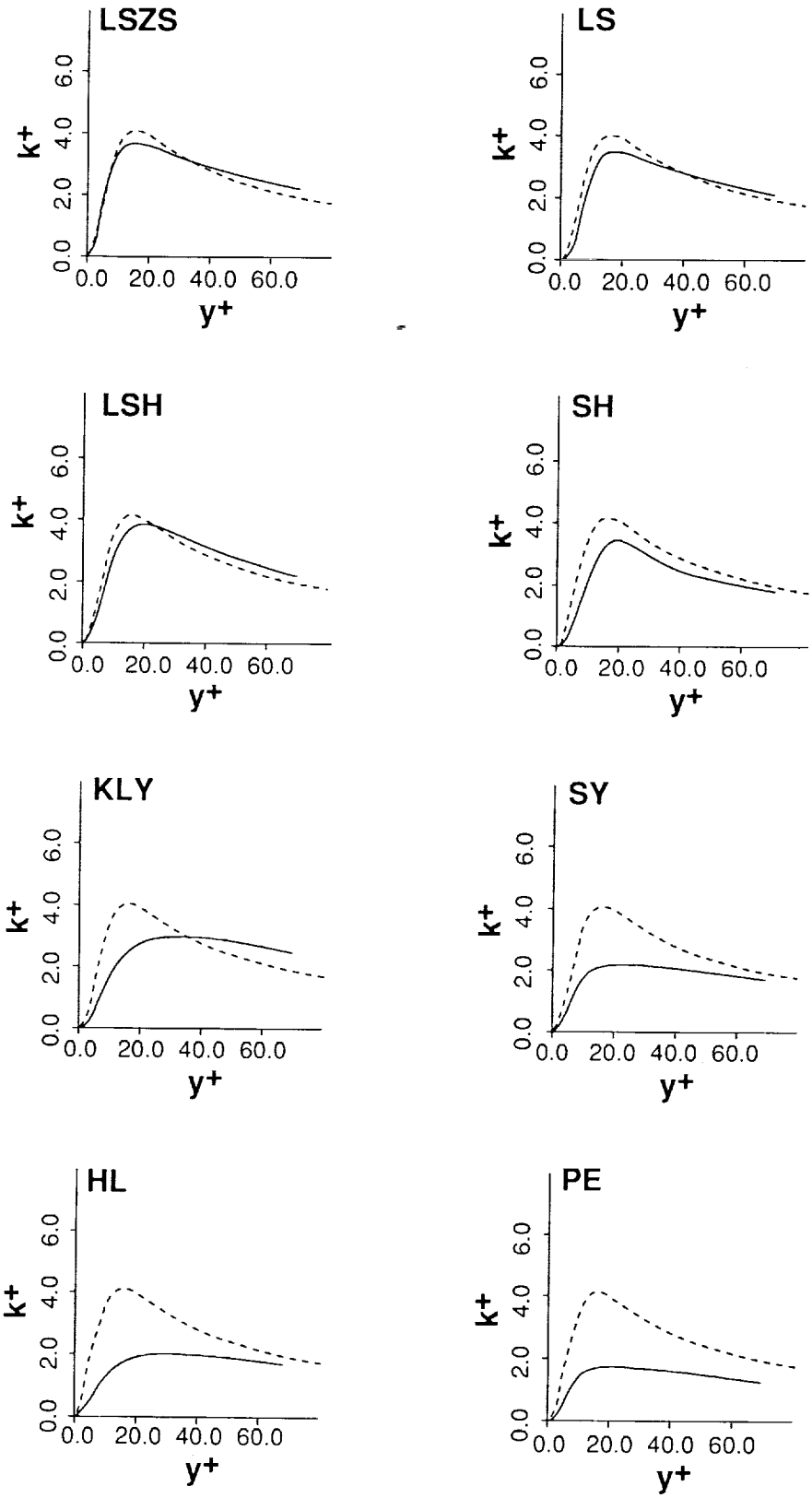

Figure 2a. Distributions of k^+ in a fully-developed channel flow: ___ model calculation; ----, direct simulation data[25]; near-wall behavior.

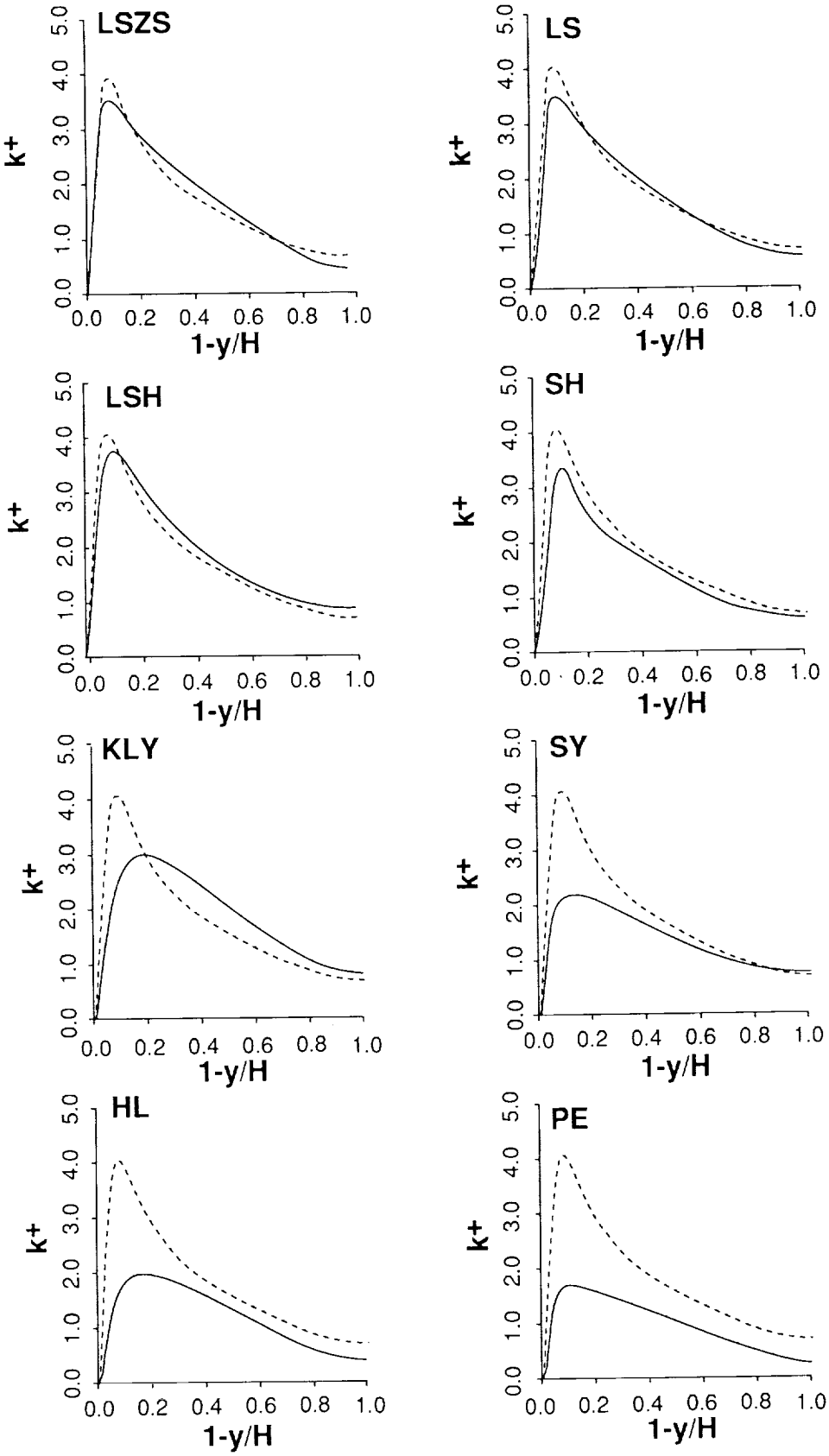

Figure 2b. Distributions of k^+ in a fully-developed channel flow: ___ model calculation; ----, direct simulation data[25]; outer flow behavior.

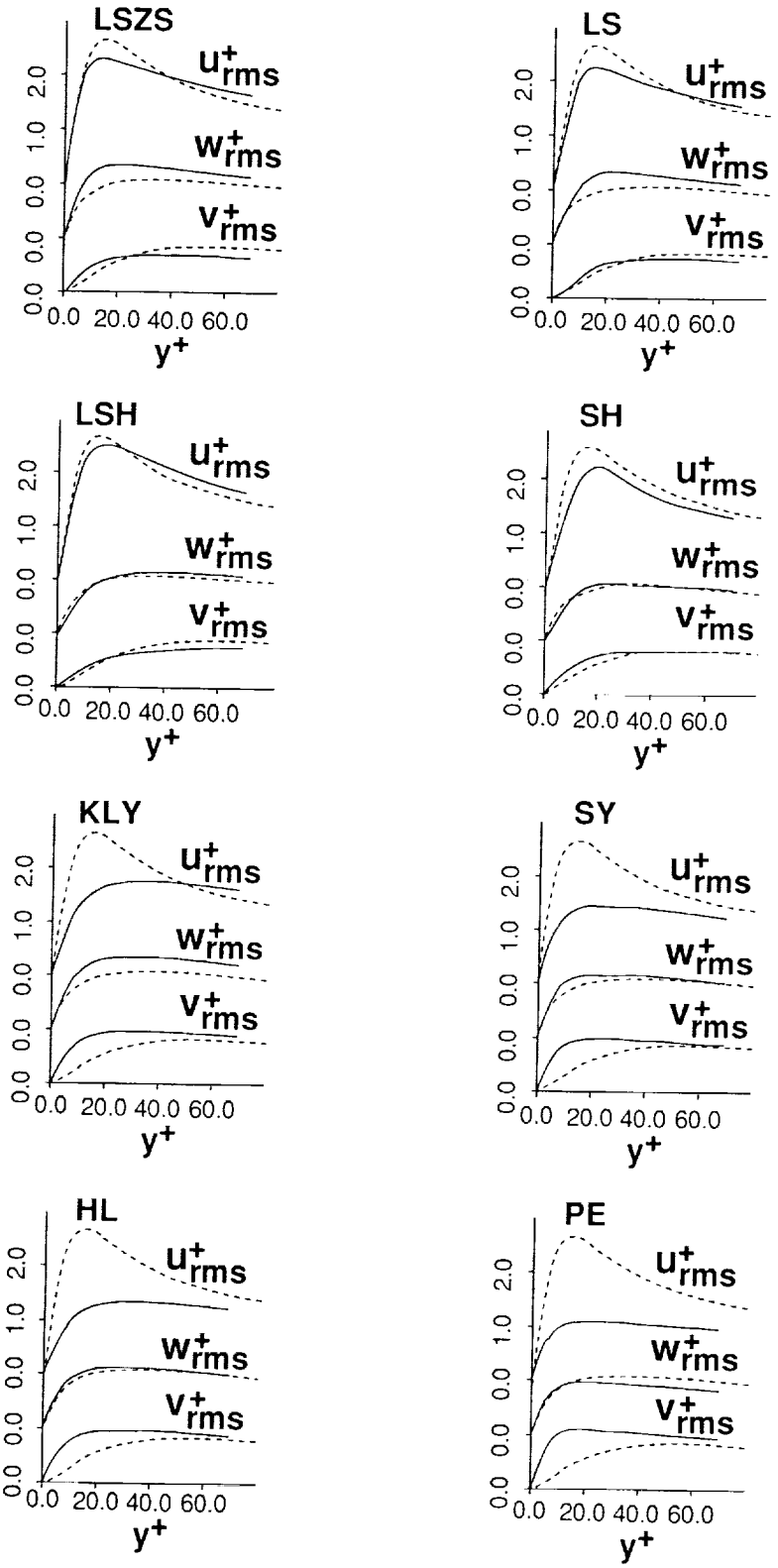

Figure 3a. Distributions of u^+_{rms}, v^+_{rms} and w^+_{rms} in a fully-developed channel flow: ___ model calculation; ----, direct simulation data[25]; near-wall behavior.

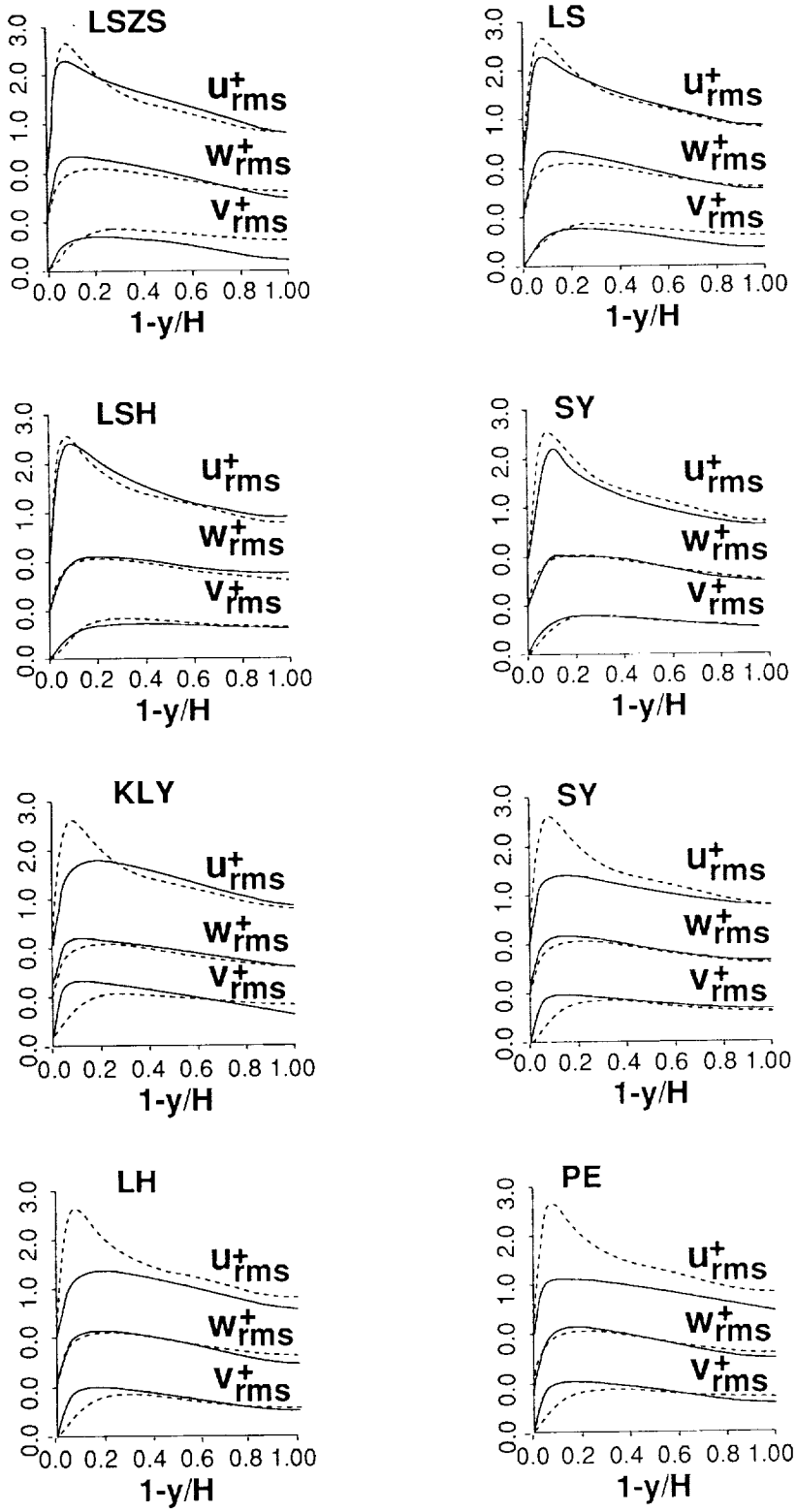

Figure 3b. Distributions of u^+_{rms}, v^+_{rms} and w^+_{rms} in a fully-developed channel flow: ___ model calculation; ----, direct simulation data[25]; outer flow behavior.

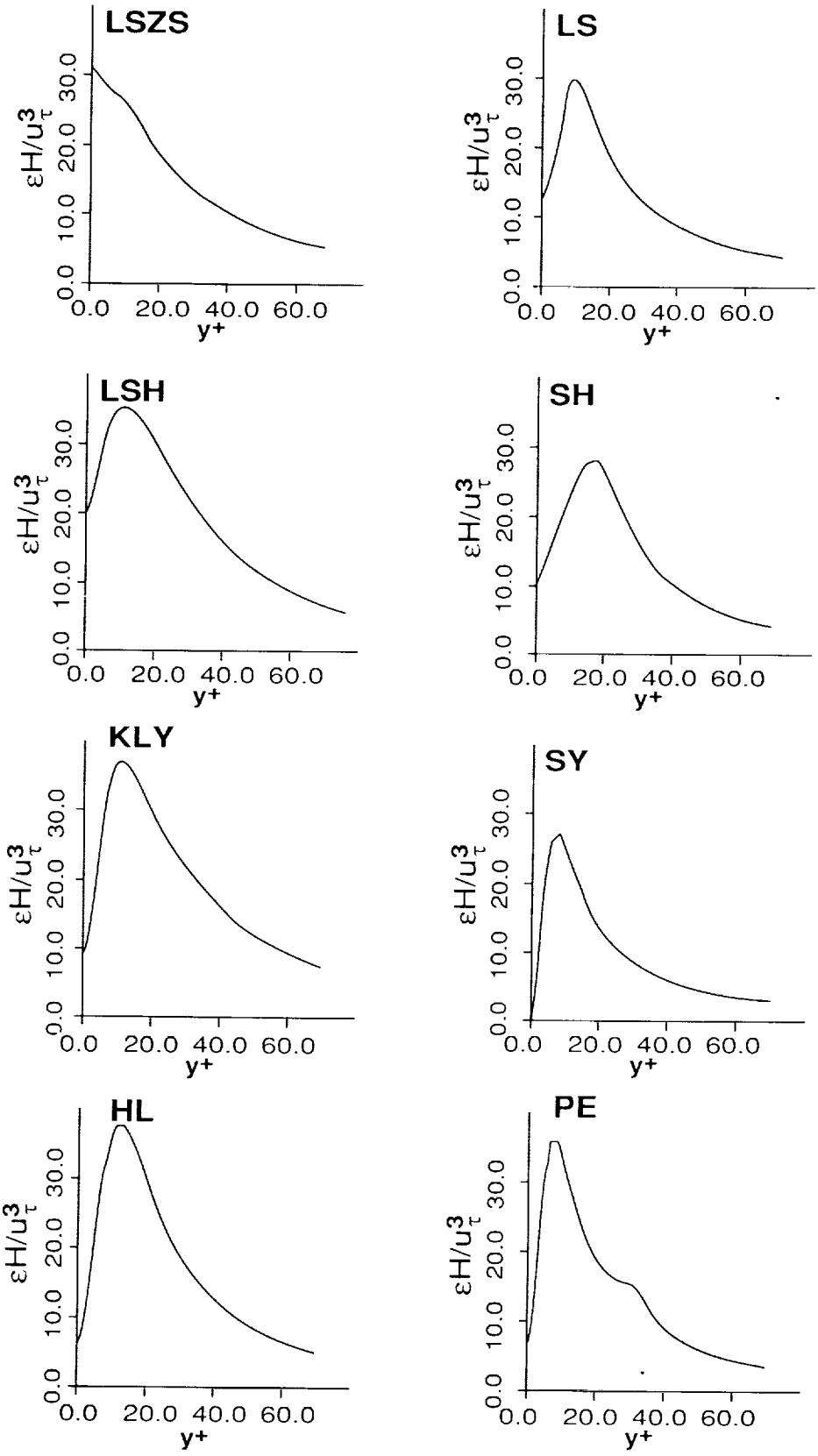

Figure 4a. Distributions of ε^+ in a fully-developed channel flow: ___ model calculation; near-wall behavior.

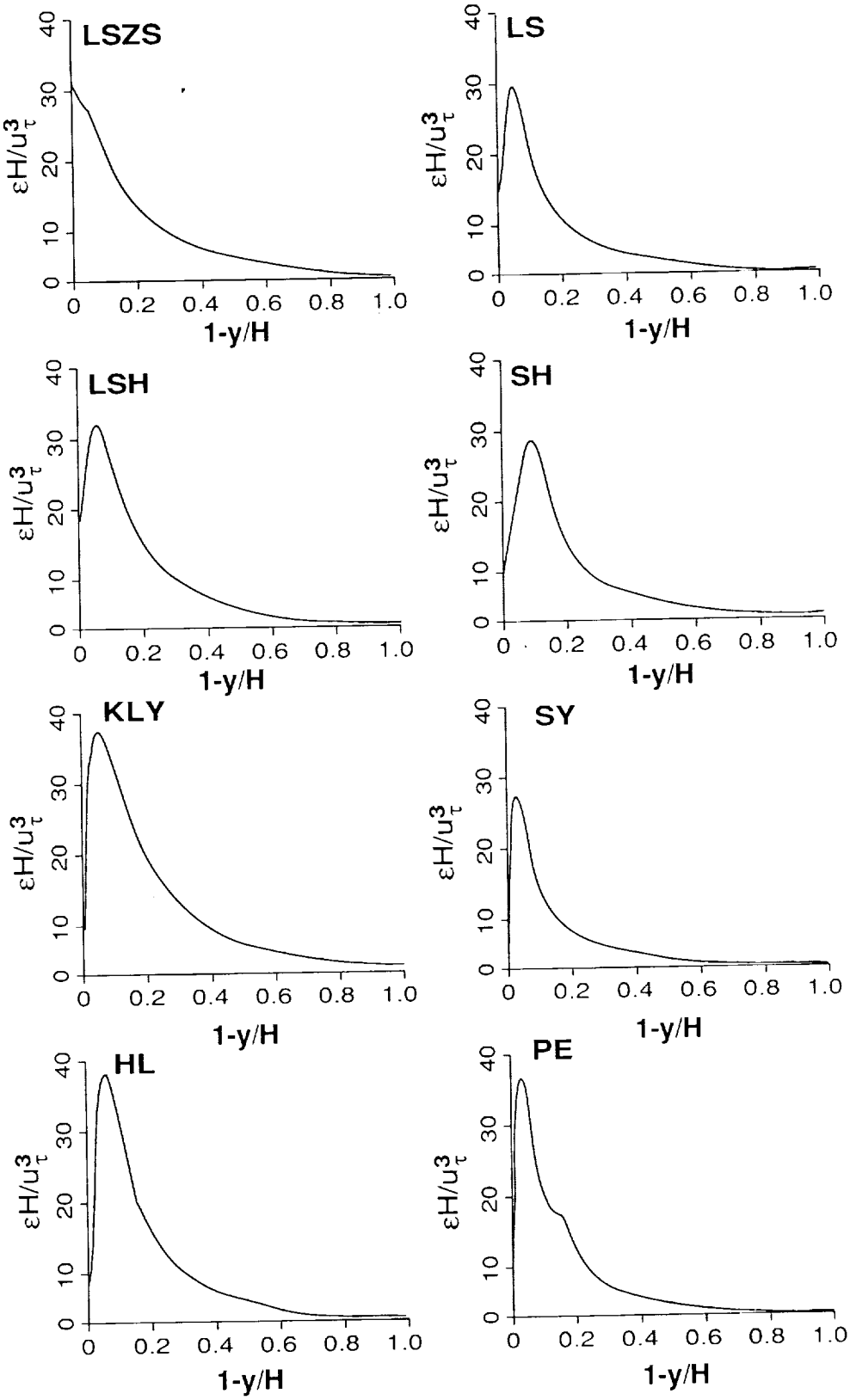

Figure 4b. Distributions of ε^+ in a fully-developed channel flow: ___ model calculation; outer flow behavior.

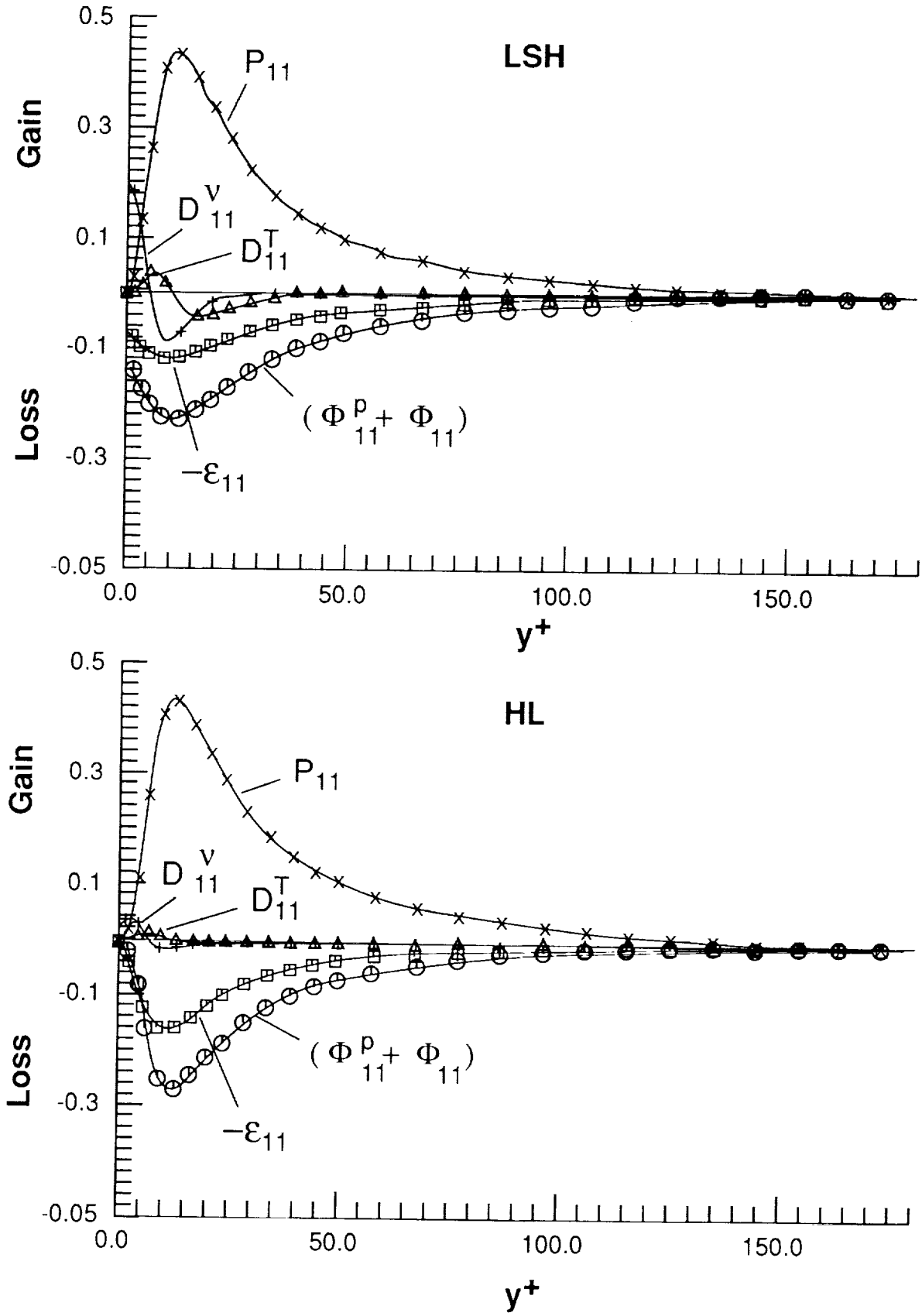

Figure 5a. The near-wall budgets of $\overline{u^2}$; HL and LSH calculations.

SO 1750/F 2a&b

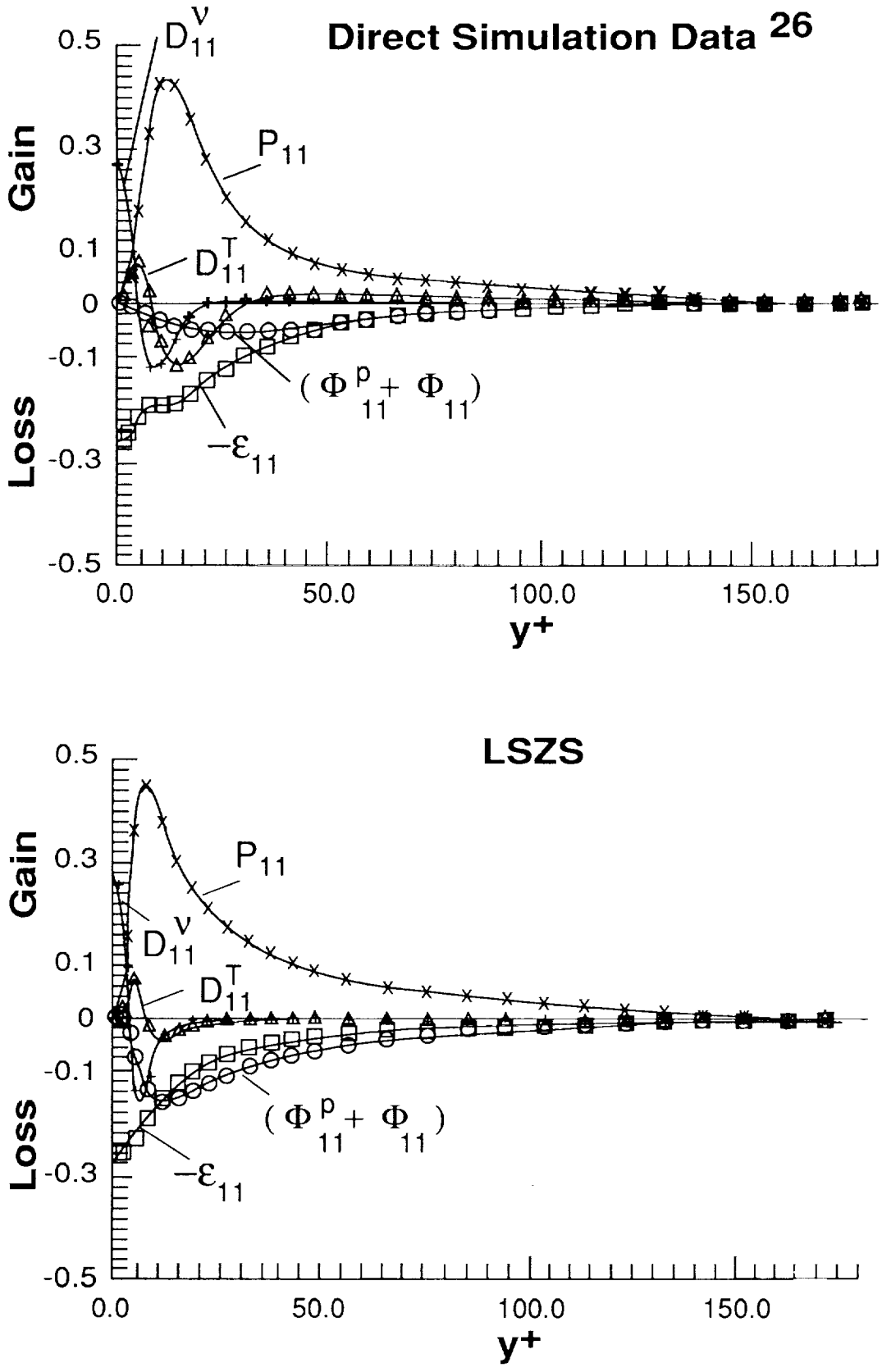

Figure 5b. The near-wall budgets of $\overline{u^2}$; LSZS calculation and data[26].

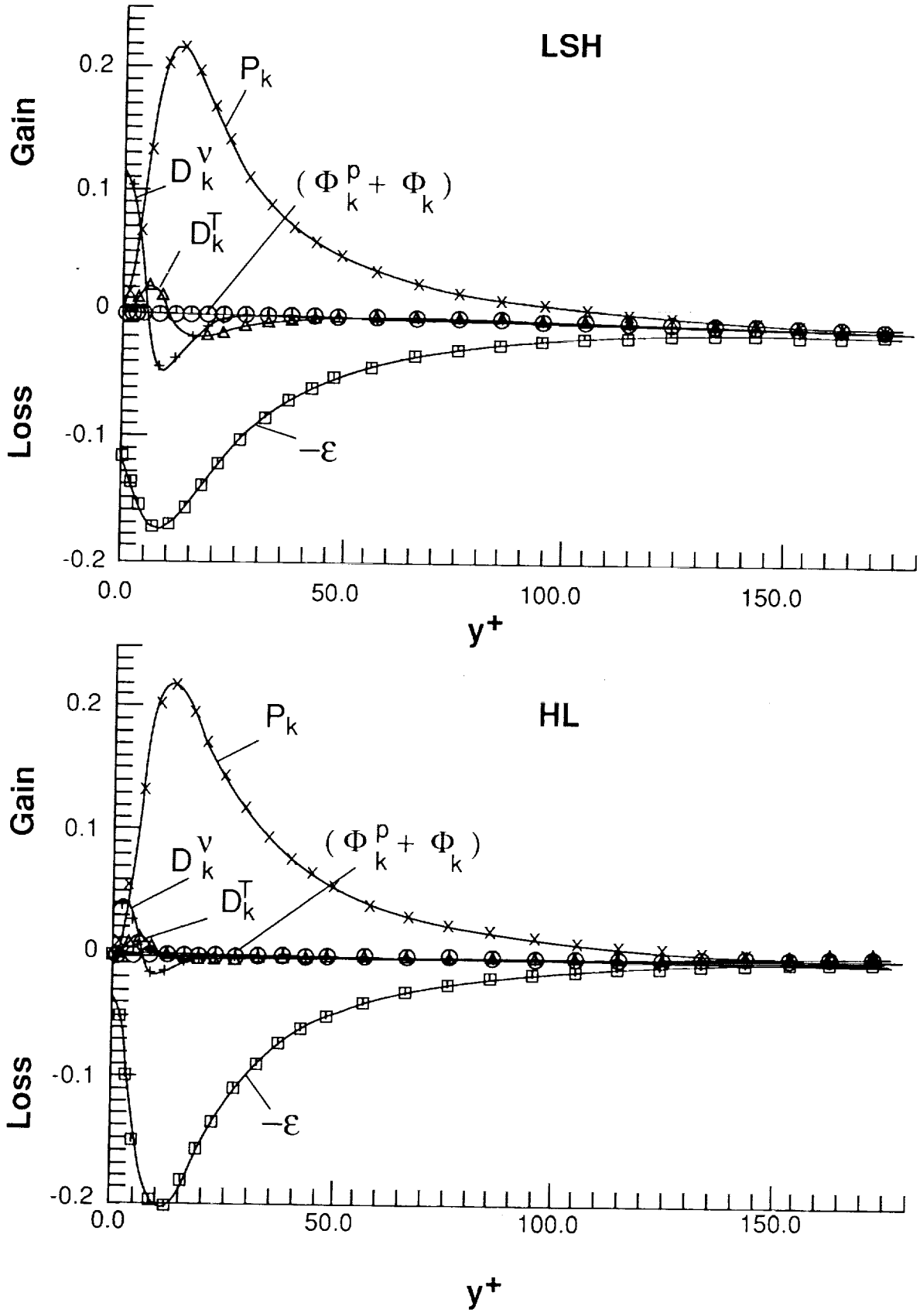

Figure 6a. The near-wall budgets of k; HL and LSH calculations.

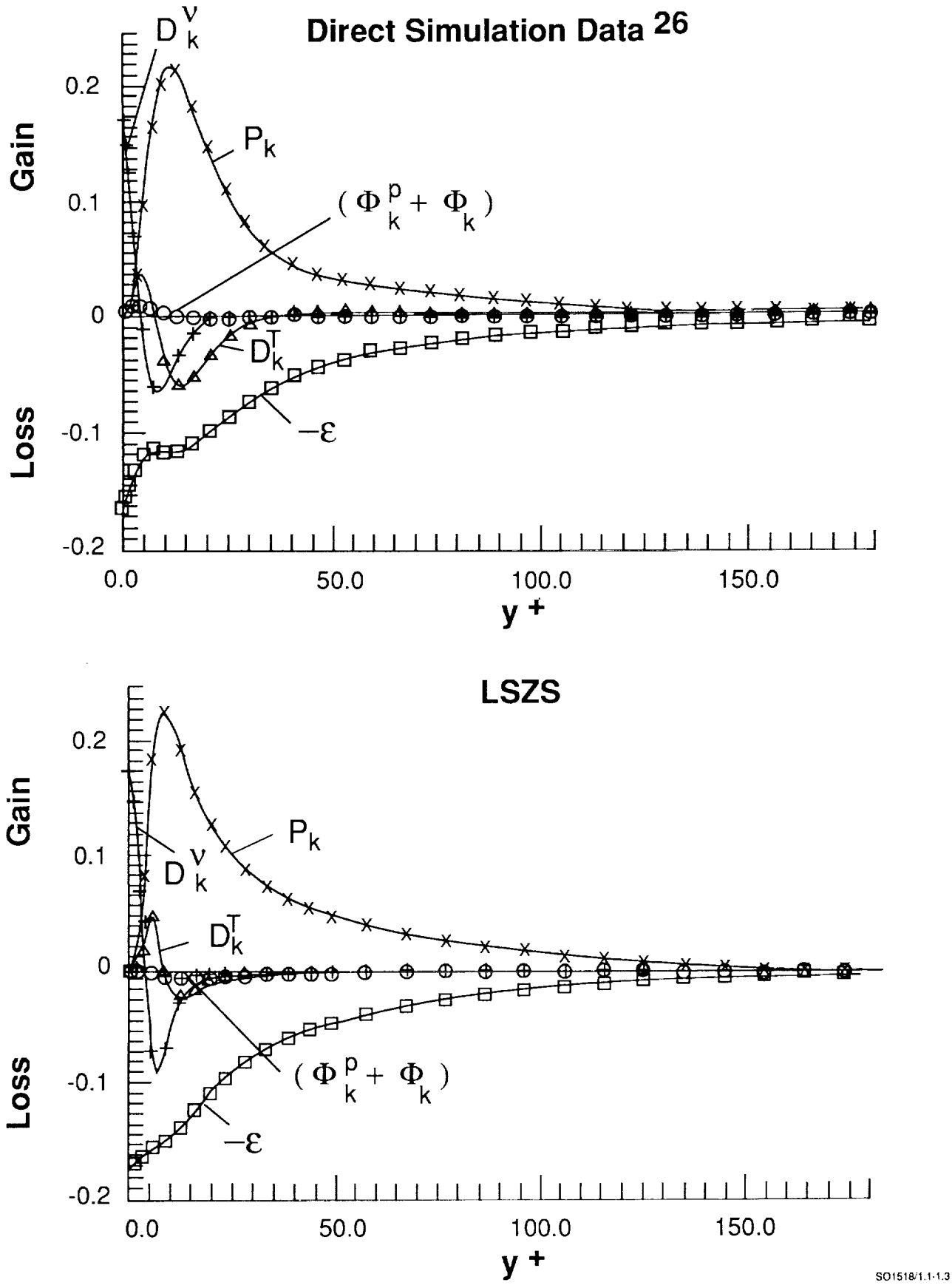

Figure 6b. The near-wall budgets of k; LSZS calculation and data[26].

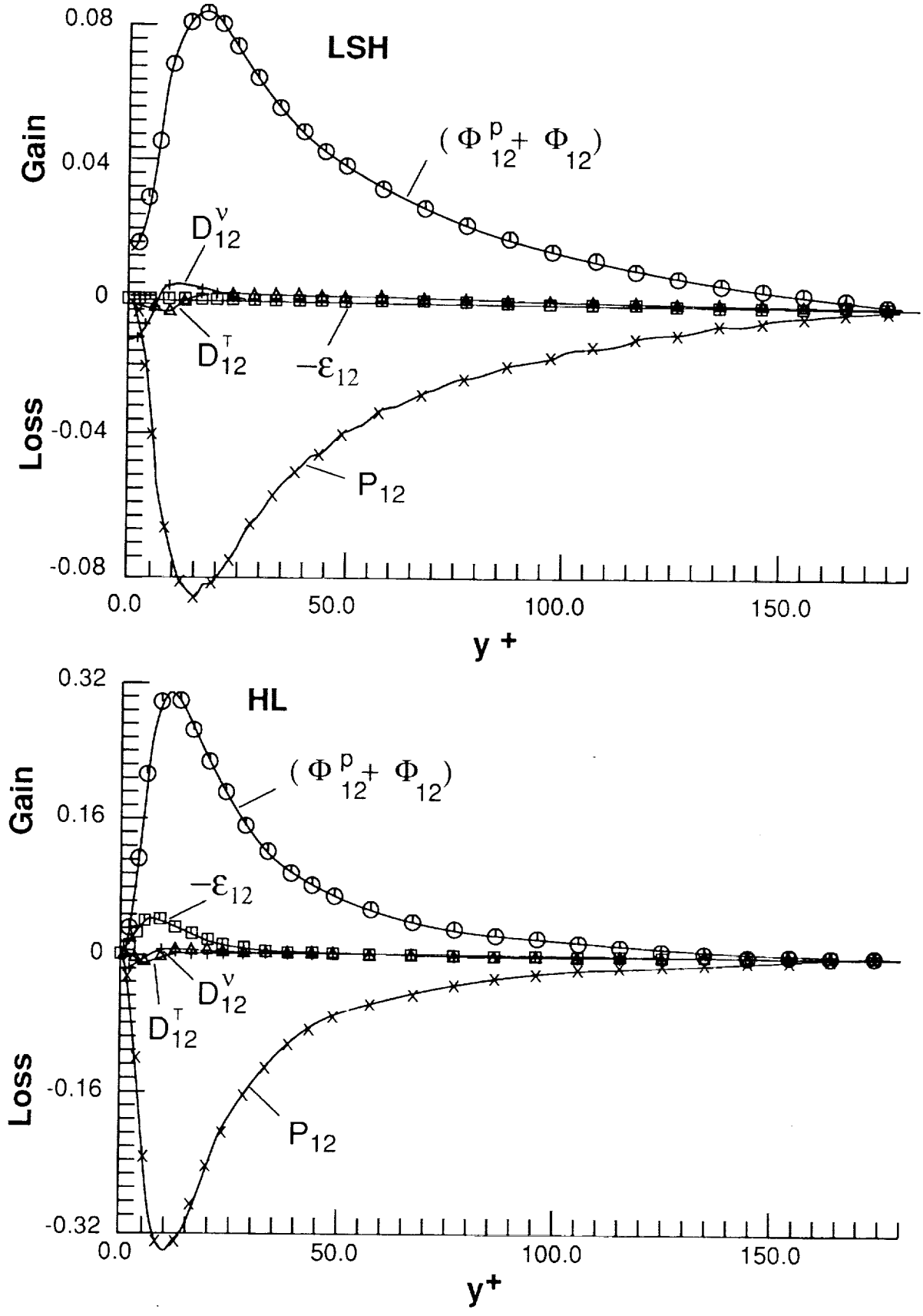

Figure 7a. The near-wall budgets of $-\overline{uv}$; HL and LSH calculations. SO1750-F 1a & b

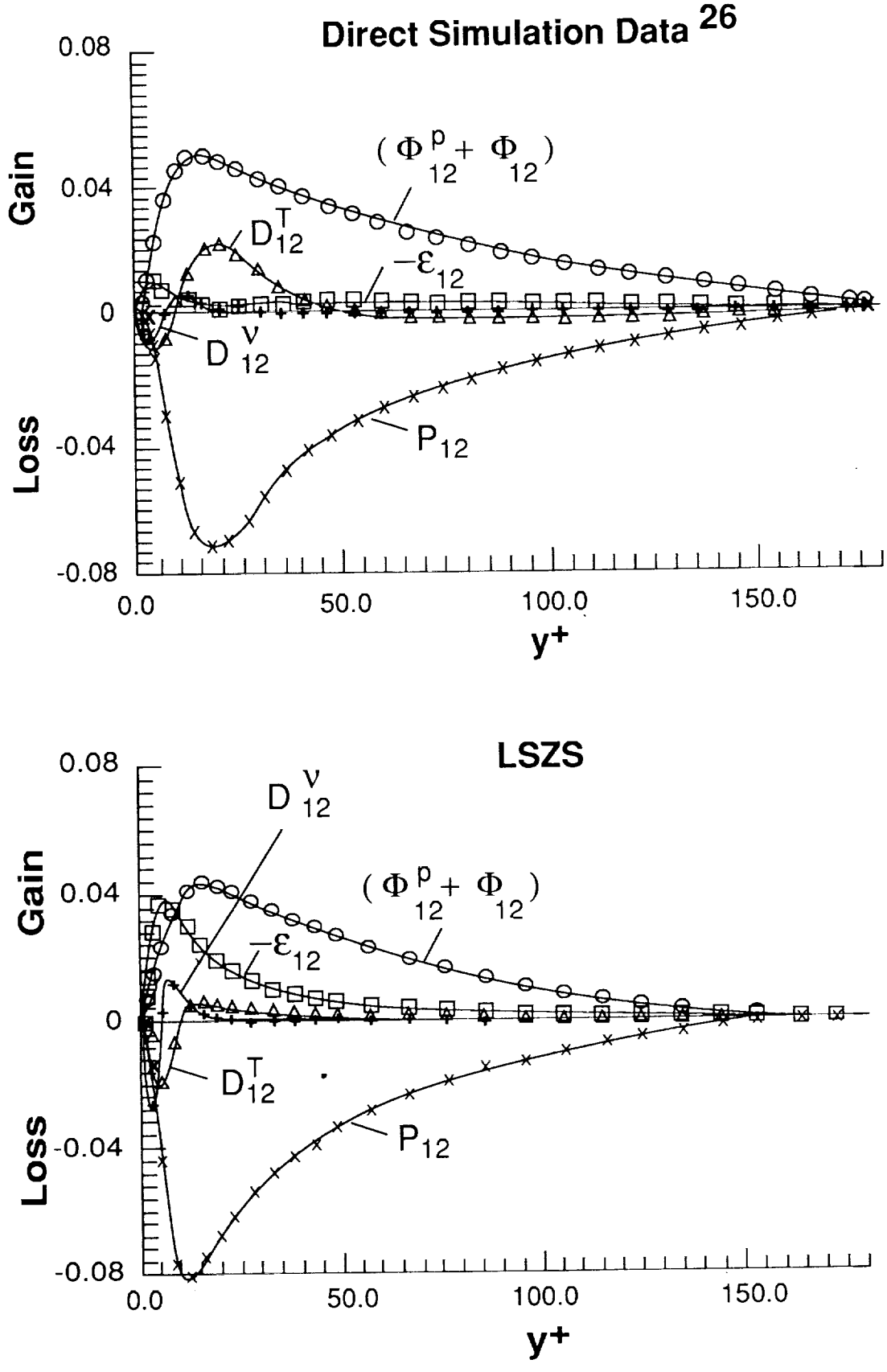

Figure 7b. The near-wall budgets of $-\overline{uv}$; LSZS calculation and data[26].

NASA
National Aeronautics and Space Administration

Report Documentation Page

1. Report No.	2. Government Accession No.	3. Recipient's Catalog No.
NASA CR-4369		

4. Title and Subtitle
A Review of Near-Wall Reynolds-Stress Closures

5. Report Date
May 1991

6. Performing Organization Code

7. Author(s)
R. M. C. So
Y. G. Lai
H. S. Zhang
B. C. Hwang*

8. Performing Organization Report No.

10. Work Unit No.
505-59-40-02

9. Performing Organization Name and Address
Arizona State University
College of Engineering & Applied Sciences
Tempe, AZ 85287-6106

11. Contract or Grant No.
NAG1-1080

13. Type of Report and Period Covered
Contractor Report

12. Sponsoring Agency Name and Address
National Aeronautics and Space Administration
Langley Research Center
Hampton, VA 23665-5225

14. Sponsoring Agency Code

15. Supplementary Notes
Langley Technical Monitor: Dr. Thomas B. Gatski
*B. C. Hwang: David Taylor Research Center, Annapolis, Maryland.

16. Abstract This paper summarizes the advances made to date in second-order near-wall turbulence closures. All closures examined are based on some form of high Reynolds-number models for the Reynolds-stress and the turbulent kinetic energy dissipation-rate equations. Consequently, most near-wall closures proposed to date attempt to modify the high-Reynolds-number models for the dissipation function, the pressure redistribution term and the dissipation-rate equation so that the resultant models are applicable all the way to the wall. The near-wall closures are examined for their asymptotic behavior so they can be compared with the proper near-wall behavior of the exact equations. A comparison of the closures' performance in the calculation of a low-Reynolds-number plane channel flow is carried out. In addition, the closures are evaluated for their ability to predict the turbulence statistics and the limiting behavior of the structure parameters compared to direct simulation data. It is found that three second-order near-wall closures give the best correlations with simulated turbulence statistics; however, their predictions of the near-wall Reynolds-stress budgets are incorrect. A proposed modification to the dissipation-rate equation remedies part of those predictions. Therefore, further improvements are required if a complete replication of all the turbulence properties and Reynolds-stress budgets by a statistical model of turbulence is desirable.

17. Key Words (Suggested by Author(s))
Turbulence models
Near-wall models
Second-order closures
Channel flow
Asymptotic behavior

18. Distribution Statement
Unclassified-Unclassified
Subject Category 02

19. Security Classif. (of this report)	20. Security Classif. (of this page)	21. No. of pages	22. Price
Unclassified	Unclassified	64	A04

For sale by the National Technical Information Service, Springfield, Virginia 22161-2171

NASA-Langley, 1991